

Clones and other interference effects in the evolution of angular momentum coherent states

P. Rozmej[†]

*Theoretical Physics Department, Institute of Physics,
University Maria Curie-Skłodowska, PL 20-031 Lublin, Poland
and
Institut des Sciences Nucléaires, F 38026 Grenoble-Cedex, France*

R. Arvieu*

*Institut des Sciences Nucléaires, F 38026 Grenoble-Cedex, France
(Received 13 January 1998, in revised form 10 July 1998)*

The aim of this article is to present the interference effects which occur during the time evolution of simple angular wave packets (WP) which can be associated to a diatomic rigid molecule (heteronuclear) or to a quantum rigid body with axial symmetry like a molecule or a nucleus. The time evolution is understood entirely within the frame of fractional revivals discovered by Averbukh and Perelman since the energy spectrum is exactly quadratic. Our objectives are to study how these interference effects differ when there is a change of the initial WP. For this purpose we introduce a two parameter set of angular momentum coherent states. From one hand this set emerge quite naturally from the three dimensional coherent states of the harmonic oscillator, from another hand this set is shown to be built from intelligent spin states. By varying one parameter (η) a scenario of interferences occur on the sphere at fractional times of the revival time that strongly depends on η . For $\eta = \pm 1$ the WP, which coincides with a WP found by Mostowski, is a superposition of Bloch or Radcliffe's states and clone exactly in time according to a scenario found for the infinite square well in one dimension and also for the two dimensional rotor. In the context of intelligent spin states it is natural to study also the evolution by changing η . For $\eta = 0$ the WP is called linear and produces in time a set of rings with axial symmetry over the sphere. The WP for other values of η are called elliptic and sets of fractional waves are generated which make a transition between two symmetries. We call 'mutants' these fractional waves. For specific times a clone is produced that stands among the mutants. Therefore the change in η produces novel change in the quantum spread on the sphere. We have also constructed simple coherent states for a symmetric rotor which are applicable to molecules and nuclei. Their time evolution also shows a cloning mechanism for the rational ratio of moments of inertia. For irrational values of this ratio, the scenario of partial revivals completed by Bluhm, Kostelecky and Tudose is valid.

I. INTRODUCTION

In the recent years one has found the existence of a generic behaviour for the time evolution of simple quantum systems. In ref. [1] Averbukh and Perelman have indeed discovered a universal scenario of fractional revivals in the long term evolution of quantum wave packets of bounded system which goes beyond the correspondence principle. They established this scenario by expanding the bound states energies relevant to the wave packet up to the second order with respect to the mean energy, thus producing a local spectrum linear plus quadratic in one quantum number. For a well concentrated wave packet at the initial time they defined two time constants T_{cl} and $T_{rev} > T_{cl}$ such that the foregoing evolution of the wave packet is predicted as follows: for $0 < t < T_{cl}$, the wave packet spreads around the mean trajectory that can be associated with the underlying classical evolution while for $T_{cl} < t < T_{rev}$ the wave packet interferes with itself in such a way that for fractional times $t = (m/n)T_{rev}$ the wave packet is divided into q fractional wave packets. If n is even, $q = n/2$, if not, then $q = n$. The specificity of the system and that of the wave packet determines the shape of the fractional wave packets which are supposed to be spread regularly around the mean trajectory. At time $t = T_{rev}$, the wave packet is rebuilt either identical or only resemblant to the original one, depending on the importance of the neglected terms higher than quadratic. In some very specific cases, the fractional wave packets are clones of the initial one as studied in the most recent paper [2] and the revival is exact. This scenario has been validated in the most spectacular manner by several authors for a wave packet in a circular orbit of the hydrogen atom [3], see also [4] and by Boris et al. [5] for an elliptic orbit. It has been extended by Bluhm and Kostelecky [6] to a very long evolution with the demonstration of superrevivals due to the cubic terms. The analytical explanation of the effects caused by cubic terms has been found by Leichtle et.al. [7]. Examples of vibrational wave packets in anharmonic potential of simple molecule were also found since [8,9]. The scenario has been thereafter extended to cases where the energy depends on two quantum numbers [10]. A recent synthesis [11] contains most of the references on this topic while ref. [12] has been devoted to the definition of the experimental of

wave packets in atomic physics and in molecular physics. The recurrences studied in ref. [1–12] are all devoted to wave packets and can be mathematically explained in terms of special Gauss’ sums. It is necessary to point out that such sums were earlier extensively used in the physical literature by Berry and Golberg [13], and Berry [14] who studied the full time evolution of the propagator of a nuclear spin with an hamiltonian of the form $l_z^2/2J$. These authors developed a renormalization theory and discussed the semiclassical limit. More recently [15] various Talbot effects (integer, fractional, fractal) were also discovered with the help of these techniques. Finally Berry [16] has shown the occurrence of fractal dimensions both in space and time during the evolution of a uniform WP in boxes of arbitrary dimensions.

Our aim is to consider only angular wave packets for diatomic molecules and also for symmetric rotors and our purpose is to discuss the time evolution of a large enough set of coherent states of the angular momentum. There is rather extensive literature on the coherent states. A full bibliography on this subject is found in ref. [17]. But we will focus on the *intelligent spin states* described in ref. [18–23] Large efforts have been made to build up such wave packets mainly in the context of group theory. Little effort, on the contrary, has been made to understand in detail their time evolution. Until the work of [1] it was not realized that they could evolve according to an universal scenario. For a diatomic molecule or for a symmetric rotor, the spectrum of which are quadratic in quantum number like for the systems discussed in [2, 24], the universal scenario is exact and repeats with period T_{rev} . The main question is whether the fractional wave packets are clones or just resemblant to the initial ones. Despite all efforts to concentrate initially the wave packet in the best possible way, the quantum evolution destroys this concentration (spatial localization) according to the rule formulated in [1]. We will show in this paper under which conditions the wave packets separate into clones and in which conditions there is a more restricted scenario of partial revivals. We will also show the existence of new fractional waves with different shapes that we call mutants. It is crucial to present a simple and physically meaningful picture of a coherent state and to decrease the number of its parameters to the minimum. One should keep in mind that a coherent wave packet has a classical content larger than the eigenstates of the angular momentum. Due to this property, it is possible to choose in the simplest manner the coherent wave packet as we will show below.

In section II we will study a large set of coherent angular WP which depend only on the angles θ and ϕ . If we impose one condition of minimum uncertainty these WP are composed of eigenstates of L^2 and contain, after a proper choice of the axis of coordinates, only spherical harmonics with magnetic quantum number m of the same parity as l . These states belong to the family of coherent states called the *intelligent spin states* [18–23]. The main body of this article is organized around a particular subset: the exponential WP which are shown to be narrowly related to the coherent states of the harmonic oscillator (see the Appendix). Moreover the angular spread of the probability density depends on a single adjustable parameter. One of the limiting case is a WP derived originally by Mostowski [25] for a diatomic molecule and is called circular. By varying one parameter one obtains new WP with cylindrical symmetry that we call linear and a large set called elliptic. Each element of this set corresponds to a quantum system like a diatomic molecule or a nucleus in a pure state with a specific preparation giving to it an average angular momentum, an angular distribution and particular spread of the distribution of the angular momentum.

In section III it will be shown that a WP obtained by Atkins and Dobson [26] using Schwinger [27] boson representation of spin 1/2 is a particular circular state almost coincident with the exponential WP. More generally the boson representation for a spin s is also shown to lead to circular states. The exponential WP provides a closed and compact expression in the angular variables.

In section IV we will state precisely for our angular WP the scenario of fractional revivals derived in [1] for the general case. It is indeed possible to specify the shape of the fractional revivals. The most spectacular event of cloning found essentially for the infinite square well in one dimension [2] and for a two dimensional rotor in [11] is extended here to the most general case of circular WP. For the linear and elliptic WP the fractional waves are generally different from the initial WP due to the quantum spread. However for a particular set of times a single clone exists which coincides with the initial WP. In the case of the most general linear WP the fractional waves keep cylindrical symmetry showing isotropy in the spread over the sphere. For the elliptic WP the fractional waves should accommodate two limiting symmetries: the plane symmetry present for circular states and the cylindrical symmetry valid for the linear states. We call ‘mutants’ these intermediate fractional waves.

In section V we present a numerical calculation showing this evolution for exponential WP. The cases where cloning occurs is somewhat obvious, however it is interesting to define properly the time windows during which a given system of clones governs the time evolution. The ‘carpet’ representation used also elsewhere [38] is an interesting tool in this respect. A second interesting result of this section lies in the shape of the mutants which can hardly be found from analytical considerations. It is found that these fractional waves preserve a good angular localization on the sphere. Their shape differs however from that of the initial WP since the generic structure is a well defined crescent-like shape.

Finally in section VI, we will construct an angular momentum coherent state of a symmetric rigid rotor according to the rules defined by Janssen [28]. The time evolution of such a state is studied in section VII. Once the number of parameters is reduced, the time evolution of the coherent state, which is now a three dimensional system with two

quantum numbers as in [10], presents clones if the ratio of the moments of inertia is rational. In the case when this ratio is not a rational number the fractional wave packets are not clones.

II. DERIVATION OF COHERENT ANGULAR WAVE PACKETS

Coherent angular WP can be defined as functions of θ and ϕ which fulfill two requirements:

1. Their angular spread should be under control i.e. it should be possible to adjust their angular distribution in the easiest manner by changing a few parameters or a simple function.
2. A criterion of minimum uncertainty should be obeyed in a manner similar to the conditions satisfied by the coherent states of the harmonic oscillator.

$$\Delta q_i \Delta p_i = \frac{\hbar}{2}, \quad i = x, y, z. \quad (1)$$

In that direction many attempts have used uncertainty relations derived with the angular variables and the angular momentum operator (see for example [17] for a complete reference to these works). Despite the long list of works devoted to this field there is no detailed evolution of the time evolution of these WP in the literature as said our introduction. The first attempts in the line of the modern developments has been done in [11] in which a WP of the rigid rotor in 2 dimensions was shown to clone exactly. Our work will extend these results to three dimensions and will discuss a rather large class of WP.

In the following we will use only uncertainty relations based upon the components of the angular momentum and we will call coherent states all the states which satisfy

$$\Delta L_x^2 \Delta L_y^2 = \frac{1}{4} \langle L_z \rangle^2. \quad (2)$$

We assume that this equation holds with the axis of coordinates such that

$$\langle L_x \rangle = 0, \quad \langle L_y \rangle = 0. \quad (3)$$

It is a textbook result that a general WP satisfies the inequality (in units with $\hbar = 1$)

$$\Delta L_x^2 \Delta L_y^2 \geq \frac{1}{4} |\langle [L_x, L_y] \rangle|^2. \quad (4)$$

This result is derived by considering the norm of the state obtained by application of a special combination of L_x with L_y which involve a real parameter called η

$$(L_x + i\eta L_y)|\Psi\rangle. \quad (5)$$

If the minimum uncertainty condition is realized there exists a value of η for which

$$(L_x + i\eta L_y)|\Psi\rangle = 0. \quad (6)$$

This value of η is related to the average values by two formulas [29]

$$\eta = \frac{\langle L_z \rangle}{2\Delta L_y^2} = \pm \sqrt{\frac{\Delta L_x^2}{\Delta L_y^2}}. \quad (7)$$

The second of these equations provides a meaningful interpretation of η in terms of ΔL_x^2 and ΔL_y^2 . Let us now construct states which satisfy eq. (6).

A. Eigenstates of L^2 .

The simplest and most natural possibility is to construct the states $|\Psi\rangle$ as eigenstates of L^2 . This problem was solved long ago [18–23] and the solutions were called *intelligent spin states*. Let us briefly sketch a few of their properties and explain why we will consider only a subset of them.

The intelligent spin states are the eigenstates $|w\rangle$ of L^2 and of the (non hermitian) operator $L_x + i\eta L_y$ with eigenvalue w such that

$$(L_x + i\eta L_y) |w\rangle = w |w\rangle. \quad (8)$$

The $(2l + 1)$ eigenvectors of (8) are discussed extensively in [19–21]. It has been shown by Rashid [21] that there is a one to one correspondance between each eigenvector $|w\rangle$ and a parent state $|lm\rangle$. Therefore instead of $|w\rangle$ it is better to denote a solution of (8) as $|\eta lm\rangle$. The relation between $|lm\rangle$ and $|\eta lm\rangle$ implies a normalisation factor a_{lm} given in [21] and an operator such that

$$|w\rangle = |\eta lm\rangle = a_{lm} \exp(\delta L_z) \exp(-i\frac{\pi}{2} L_y) |lm\rangle. \quad (9)$$

The parameter δ is related to η by

$$\exp(\delta) = \sqrt{\frac{1 + \eta}{1 - \eta}}, \quad (10)$$

and the eigenvalue w is expressed in terms of m by

$$w = m \sqrt{1 - \eta^2}. \quad (11)$$

Among the $2l + 1$ states (9) one can identify:

1. The states with $m = 0$ which fulfill eq. (2) and (3). These states will be taken into account and will be explicated thereafter.
2. The states with $m = \pm 1$. These particular states were first introduced by Bloch and Radcliffe [18]. In a more convenient system of coordinates they fulfill the simpler equation with $\eta = 1$ [20, 21]

$$(L_x + i L_y) |w\rangle = 0. \quad (12)$$

Therefore these states will also be considered in our paper and we will call them circular states.

3. The states for which the parent value m is neither 0 or ± 1 . These states do not coincide with the previous ones. However they are not orthogonal to them. Moreover they require a value of l larger or equal to 2 i.e. a tensor of rank at least equal to two is needed in order to generate them. We have not studied these states and it is still an open question to build a convenient WP by implying them.

On the contrary the states with $m = 0$ can be generated quite naturally starting from a three dimensional gaussian WP as shown in the Appendix and require a very simple vector operator. The states with $m = 0$ have a very simple structure in terms of spherical harmonics that is worth to be presented shorly independently on the general solution found in [21]. Let us denote by $\mathcal{Y}_\eta^l(\theta, \phi)$ these new spherical harmonics which depend on a continuous real parameter η and let us expand them in terms of the usual Y_m^l as

$$\mathcal{Y}_\eta^l(\theta, \phi) = \sum_{m=-l}^l C_m^l(\eta) Y_m^l(\theta, \phi). \quad (13)$$

The recurrence between the C_m^l derived from eq. (6) implies that the sum (13) is restricted in such a way that m and l have the same parity, indeed the recurrence is:

$$C_{m+1}^l = -C_{m-1}^l \frac{1 + \eta}{1 - \eta} \sqrt{\frac{l(l+1) - m(m-1)}{l(l+1) - m(m+1)}}. \quad (14)$$

In the following we will need the expression of \mathcal{Y}_η^l for $l = 1$ which is

$$\begin{aligned}\mathcal{Y}_\eta^1(\theta, \phi) &= \frac{(1+\eta)Y_1^1 - (1-\eta)Y_{-1}^1}{\sqrt{2(1+\eta^2)}} \\ &= -\frac{1}{4}\sqrt{\frac{3}{\pi}}\frac{1}{\sqrt{1+\eta^2}}\sin\theta(\cos\phi + i\eta\sin\phi).\end{aligned}\tag{15}$$

The combination of θ , ϕ and η given above will be defined as

$$v = \sin\theta(\cos\phi + i\eta\sin\phi).\tag{16}$$

One has

$$\langle \mathcal{Y}_\eta^1 | L_z | \mathcal{Y}_\eta^1 \rangle = \frac{2\eta}{1+\eta^2}.\tag{17}$$

Similarly, for $l = 2$ the coherent states are

$$\mathcal{Y}_\eta^2(\theta, \phi) = \left[\frac{8}{3}(1+\eta^4) + \frac{32}{3}\eta^2 \right]^{-1/2} \left\{ (1+\eta)^2 Y_2^2 - \sqrt{\frac{2}{3}}(1-\eta^2)Y_0^2 + (1-\eta)^2 Y_{-2}^2 \right\},\tag{18}$$

while the average of L_z is

$$\langle \mathcal{Y}_\eta^2 | L_z | \mathcal{Y}_\eta^2 \rangle = \frac{6\eta(1+\eta^2)}{1+4\eta^2+\eta^4}.\tag{19}$$

It is interesting to point out that $\eta = \pm 1$ corresponds to states with $m = \pm l$ while the states with $l = 0$ are eigenstates of L_x and can be more simply written as single spherical harmonics of the angle θ' defined as

$$\cos\theta' = \sin\theta\cos\phi,\tag{20}$$

and one has

$$\mathcal{Y}_0^l(\theta, \phi) = Y_0^l(\theta', \phi') = \sum_{m=-l}^l C_m^l(0) Y_m^l(\theta, \phi).\tag{21}$$

The coherent spherical harmonics $\mathcal{Y}_\eta^l(\theta, \phi)$ have no freedom in them which allows a proper angular localization. It is therefore necessary to consider linear combinations.

B. General WP.

The most general WP solutions of (6) which fulfill eq. (2) will be written as

$$|\Psi_\eta\rangle_{\text{general}} = \sum_l \lambda_\eta^l |\mathcal{Y}_\eta^l\rangle.\tag{22}$$

They depend on η which can be interpreted with the help of eq. (7) and on weights λ^l which can be determined in order to provide a convenient angular localization. Again there will be states with $\eta = \pm 1$ that will be called circular and others with $\eta = 0$ that will be called linear. The WP defined with other values of η will be called elliptic in the following. The justification of this name will be given in the Appendix. In section III many results will be derived for the particular class of WP that will be defined in the following subsection. Most of them can be seen to apply to the general WP (22).

C. Exponential coherent WP.

Among functions that are possible those which can be expanded in a power series of the variable v defined by (16) are particularly interesting because they will contain all the partial waves \mathcal{Y}_η^l . We have chosen to concentrate on the exponential coherent WP

$$\Psi_\eta(\theta, \phi) = \sqrt{\frac{N}{2\pi \sinh 2N}} e^{N \sin \theta (\cos \phi + i\eta \sin \phi)}, \quad (23)$$

which possess important properties: they fulfil eq. (2), they have direct connection to coherent states of harmonic oscillator (see the Appendix) and finally they have a simple geometrical interpretation. Indeed the real parameter N introduced there allows a proper adjustment of the angular spread. The probability density depends only on N and on the angle θ' defined by (20), the expression is

$$|\Psi_\eta(\theta, \phi)|^2 = \frac{N}{2\pi \sinh 2N} e^{2N \cos \theta'}. \quad (24)$$

If we put $\eta = 1$ into (18) we obtain a coherent state defined by Mostowski [25] who wrote it as

$$\Psi_M(\theta, \phi) = C^{-\frac{1}{2}} e^{N(\vec{u}_1 + i\vec{u}_2) \cdot \vec{n}}. \quad (25)$$

Here \vec{u}_1 and \vec{u}_2 are two perpendicular unit vectors (in our case \vec{u}_1 is along Ox and \vec{u}_2 along Oy and we have eq. (3) and \vec{n} is a unit vector in the direction (θ, ϕ) .

The generalization of (25) with a parameter η was never considered until now to our knowledge and the time evolution was never studied yet. Let us point out that eq. (23) can be generalized as

$$\Psi_\eta(\theta, \phi) = C^{-\frac{1}{2}} e^{N(\vec{u}_1 + i\eta\vec{u}_2) \cdot \vec{n}} \quad (26)$$

with arbitrary but perpendicular \vec{u}_1 and \vec{u}_2 . Calling \vec{u}_3 a third unit vector perpendicular to \vec{u}_1 and \vec{u}_2 we will obtain WP which do not fulfill eq. (2) but rather

$$\Delta L_1^2 \Delta L_2^2 = \frac{1}{4} \langle L_3 \rangle^2. \quad (27)$$

Instead of eq. (3) we would have

$$\langle L_1 \rangle = 0, \quad \langle L_2 \rangle = 0. \quad (28)$$

The choice of axis made in eq. (23) simplifies much the interpretation and the partial wave expansion. This expansion will be given in subsection IID.

It is not difficult to derive that our Ψ_η defined by (23) have the following average values and the following limits for large N :

$$\langle \Psi_\eta | L_z | \Psi_\eta \rangle = \langle L_z \rangle = \eta [N \coth(2N) - \frac{1}{2}] \xrightarrow{N \rightarrow \infty} \eta [N - \frac{1}{2}]. \quad (29)$$

Therefore eq. (7) implies that

$$\Delta L_y = \langle L_y^2 \rangle = \frac{1}{2} [N \coth(2N) - \frac{1}{2}] \xrightarrow{N \rightarrow \infty} \frac{1}{2} [N - \frac{1}{2}], \quad (30)$$

$$\Delta L_x = \langle L_x^2 \rangle = \frac{\eta^2}{2} [N \coth(2N) - \frac{1}{2}] \xrightarrow{N \rightarrow \infty} \frac{\eta^2}{2} [N - \frac{1}{2}]. \quad (31)$$

The average of L_z^2 and the total uncertainty ΔL_η^2 need independent calculations with the results:

$$\langle L_z^2 \rangle = \langle L_y^2 \rangle [1 - 2\eta^2] + \eta^2 N^2, \quad (32)$$

$$\Delta L_\eta^2 = \langle L^2 \rangle - \langle L_z \rangle^2 \xrightarrow{N \rightarrow \infty} N - \frac{1}{2} + \eta^2 \frac{N}{2}. \quad (33)$$

D. Partial wave expansion of the exponential coherent state.

We need to distinguish the case with a general value of η from the simpler cases with $\eta = 1$ or 0 . (The cases with $\eta = -1$ or negative η are trivially deduced from the cases with positive η by inverting the sense of rotation of the WP). For $\eta = 1$, i.e. circular exponential WP, or Mostowski's WP one has

$$\Psi_M(\theta, \phi) = \Psi_1(\theta, \phi) = \sqrt{\frac{2N}{\sinh 2N}} \sum_{I=0}^{\infty} \frac{(2N)^I}{\sqrt{(2I+1)!}} Y_I^I(\theta, \phi). \quad (34)$$

For $\eta = 0$, i.e. linear exponential WP, it is found that

$$\Psi_0(\theta, \phi) = \Psi_0(\theta', \phi') = \sqrt{\frac{N}{2\pi \sinh 2N}} e^{N \cos \theta'} \quad (35)$$

$$= \sqrt{\frac{2N}{\sinh 2N}} \sum_{I=0}^{\infty} \sqrt{2I+1} \sqrt{\frac{\pi}{2N}} I_{I+\frac{1}{2}}(N) Y_0^I(\theta', \phi'), \quad (36)$$

where $I_{I+\frac{1}{2}}(N)$ is a spherical Bessel function of the first kind.

For a general value of η , i.e. elliptic WP, the argument v can be separated into two parts

$$v = \frac{1+\eta}{2} \sin \theta e^{i\phi} + \frac{1-\eta}{2} \sin \theta e^{-i\phi}. \quad (37)$$

Then e^{Nv} is calculated as two power series containing products of Y_l^l and Y_{-l}^l . These products are then expanded in terms of Y_M^I as

$$\Psi_\eta(\theta, \phi) = \sum_{IM} b_{IM}(N, \eta) Y_M^I(\theta, \phi), \quad (38)$$

with the weights b_{IM} given by

$$b_{IM}(N, \eta) = \sqrt{\frac{2N}{\sinh(2N)}} \sum_{l'l'} \frac{(-1)^{l'} [N(1+\eta)]^l [N(1-\eta)]^{l'}}{\sqrt{(2l)!(2l')!}} \frac{\langle ll'00|I0\rangle \langle ll'l-l'|IM\rangle}{\sqrt{2I+1}}. \quad (39)$$

From the discussion made in subsection II A b_{IM} is proportional to C_{IM} . The known selection rules of the Clebsch-Gordan coefficients which appear in (39) assure that M should have the parity of I .

III. COMPARISON WITH COHERENT STATES DEFINED IN TERMS OF BOSONS

In this section we will compare the previous coherent states to an other set defined in terms of bosons of spin s . Based on Schwinger's work [27] several angular momentum coherent states have been constructed which rely upon boson representation of spin s . The case with $s = 1/2$ was first considered by Bonifacio et al. [33] and studied more extensively by Atkins and Dobson [26]. Mikhailov [34] has generalized this case to any spin integer or half integer. His work was complemented by Gulshani [35]. According to Mikhailov, a coherent state formed with $2s + 1$ bosons depends on 2 complex numbers called α_+ and α_- combined to define other complex constants α_{jm} by

$$\alpha_{jm} = \alpha_+^{j+m} \alpha_-^{j-m} \binom{2j}{j-m}^{\frac{1}{2}}, \quad (40)$$

for $j = 0, s, 2s, \dots, ps, \dots$ and $m = -j, -j+1, \dots, j-1, j$.

The coherent state, called generically $|\alpha s\rangle$, is expressed by

$$|\alpha s\rangle = \exp\left(-\frac{n^{2s}}{2}\right) \prod_{\mu} \exp(\alpha_{s\mu} a_{\mu}^{\dagger}) |0\rangle \quad (41)$$

$$= \exp\left(-\frac{n^{2s}}{2}\right) \sum_{j=0, s, \dots, ps, \dots}^{\infty} \sum_{m=-j}^j \frac{1}{\sqrt{j!}} \alpha_{jm} |jms\rangle, \quad (42)$$

$|0\rangle$ represents the vacuum, a_μ^\dagger ($\mu = -s, \dots, s$) is a creation operator of a boson of spin s , while the normalization constant depends on α_+ and α_- through

$$n^{2s} = (|\alpha_+|^2 + |\alpha_-|^2)^{2s} = \sum_\mu |\alpha_{s\mu}|^2. \quad (43)$$

The states $|jms\rangle$ are normalized states of angular momentum j constructed from the a_μ^\dagger [see Mikhailov for the full expressions]. The expansion (42) contains integer and half integer j for $s = 1/2$, it reduces to integer j for $s = 1$, for $s = 2$ only even j occurs etc. The states (41)–(42) are eigenstates of the annihilation operator a_μ^\dagger ($\mu = -s \dots + s$) with eigenvalue $\alpha_{s\mu}$. Mikhailov has also calculated the expectation values of various operators which are expressed in terms of a_μ^\dagger and a_μ . Due to this technical simplification, the calculations of expectation values are easier than the work necessary to obtain formulas (29) to (33) in the case of the coherent state $\Psi_\eta(\theta, \phi)$. It is interesting to compare the properties of the state $|\alpha s\rangle$ to those of the general state defined by eq. (22) or to (23). Since α_{jm} is generally non zero for all values of j and m the states $|\alpha s\rangle$ cannot be identified with our elliptic state for which m should be of the same parity as j . Clearly formulas (40) and (39) are different. At first sight one could think that (41) which depend on s and on two complex numbers α_+ and α_- describe an ensemble of WP larger than our WP (23) which depend only on N and η and would therefore apply to a larger variety of physical situations. We will show that on the contrary the states (41) are a particular set of circular states and do not contain the freedom allowed with the parameter η . Indeed if α_+ and α_- are both nonzero the states (41) do not fulfill the conditions (3). In order to fulfill these conditions it is necessary that either α_+ or α_- should be zero. [In [34] it is shown indeed that $\langle L_x \rangle \sim \text{Re}(\alpha_+^* \alpha_-)$, $\langle L_y \rangle \sim \text{Im}(\alpha_+^* \alpha_-)$]. A change of axis leads to $\alpha_{jm} = 0$ except if $m = j$ (if $\alpha_- = 0$) or if $m = -j$ (if $\alpha_+ = 0$). The phase of α_+ or α_- can be incorporated in the phase of the states $|j, m = \pm j, s\rangle$. Choosing for example $\alpha_- = 0$ and $\alpha_+ = k = \text{real number}$ the state $|\alpha s\rangle$ is now simply denoted as $|ks\rangle$

$$|ks\rangle = \exp\left[-\frac{(k^2)^{2s}}{2}\right] \sum_{j=0, s, \dots, ps, \dots}^{\infty} \frac{1}{\sqrt{p!}} (k^2)^j |j = ps, m = j, s\rangle \quad (44)$$

$$= \exp\left(-\frac{k^{4s}}{2}\right) \exp[\alpha_{ss} a_s^\dagger] |0\rangle. \quad (45)$$

In the previous section, it was clear from the compact expression (25) given by Mostowski that the same physical state can be written by introducing three additional angles which are necessary to specify \vec{u}_1 and \vec{u}_2 . The proof that this freedom exists also in the boson representation was given by Mikhailov [34]. By a convenient choice of axis the state written in eq. (42) with $2s + 1$ bosons and two complex parameters can be brought to the simple form (44-45) with only one boson of spin s with $\mu = s$ and one parameter $\alpha_{ss} = \alpha_+^{2s} = k^{2s}$. Such a choice was also done by Atkins and Dobson [26] for the case $s = 1/2$. The matrix elements of the components of \vec{L} given below are a particular case of formulas given in ref. [26].

$$\langle ks | L_z | ks \rangle = s k^{4s}, \quad (46)$$

$$\langle ks | L_z^2 | ks \rangle = s^2 k^{4s} (k^{4s} + 1), \quad (47)$$

$$\langle ks | L_x^2 | ks \rangle = \langle ks | L_y^2 | ks \rangle = \frac{s}{2} k^{4s}, \quad (48)$$

$$\Delta L_x^2 \Delta L_y^2 = \frac{1}{4} \langle L_z \rangle^2. \quad (49)$$

These formulas and expansion (44-45) compared to formulas (29) to (32) show that $|ks\rangle$ do not coincide exactly with Mostowski's coherent state. For $s = 1/2$ Atkins and Dobson have proposed to truncate the sum over j in order to take into account only integer values of j . In this process the new state that we will call $|k, \frac{1}{2}\rangle_i$ (i for integer) needs to be normalized properly and the formulas (46) to (48) cease to be valid. Eq. (49) still holds because the state is nevertheless a circular state.

Our purpose is now to compare $\Psi_M(\theta, \phi)$ to $|k, \frac{1}{2}\rangle_i$. It is interesting to choose the parameters N and k in such a way that the limit (29) for large N is valid ($\eta = 1$). Then using (46) one puts

$$\frac{1}{2} k^2 = N - \frac{1}{2}. \quad (50)$$

The comparison presented in Fig. 1 shows that the probability C_I^2 to find the partial wave Y_I^I in Ψ_M and in $|k, \frac{1}{2}\rangle_i$ is practically the same for $N = 20$. For smaller N and k (i.e. N of the order of unity) we have observed small but not meaningful differences. It is therefore possible, if N is large enough, to identify Mostowski's coherent state to the boson representation of spin 1/2 of Atkins and Dobson.

We have shown in this section that the coherent states derived in the literature using a boson representation belongs to the particular class of coherent circular states defined in section II. The exponential coherent states defined in subsection II C above have the advantage of a well controllable localization and also depends on an interesting new parameter η .

IV. TIME EVOLUTION OF COHERENT ANGULAR WP

The coherent states built in section II are applicable to systems which have only angular coordinates on the sphere. This is the case of the three dimensional rotor with an axis of symmetry like an heteronuclear molecule or some deformed nuclei. In the following we will assume that the eigenvalues of these systems obey rigorously the $I(I+1)$ law and we will use the frequency ω_0 written in terms of the moment of inertia J_0 as

$$\omega_0 = \frac{\hbar}{2J_0}. \quad (51)$$

Our WP do not allow to consider other degrees of freedom like vibrational ones or internal excitations. However we are confident of the interest of our work which provides a full quantum-mechanical description of the rotation of a pure state of a three dimensional system.

Let us define the *revival time*, T_{rev} as

$$T_{rev} = \frac{2\pi}{\omega_0} = (2\bar{I} + 1) T_{cl}. \quad (52)$$

This time is twice the period of true revival of the WP. Indeed one has for the general case (22)

$$\Psi_\eta(\theta, \phi, t)_{general} = \sum_I \lambda_I e^{-i2\pi I(I+1)\omega_0 t} \mathcal{Y}_\eta^I(\theta, \phi) \quad (53)$$

Since $I(I+1)$ is always even the period is indeed $T_{rev}/2$. Nevertheless we will continue to use the same notations as in [1]. These authors have also introduced a second characteristic time T_{cl} called the *classical time*. It is defined in terms of the average angular momentum \bar{I} defined by the average energy of the WP

$$\bar{I}(\bar{I} + 1) = \sum_I |\lambda_I|^2 I(I + 1) \quad (54)$$

For the case of an exponential WP one obtains with the help of eqs. (30-32):

$$\bar{I}(\bar{I} + 1) = \langle L^2 \rangle \xrightarrow{N \rightarrow \infty} \left(N - \frac{1}{2} \right) + \eta^2 \left[N^2 - \frac{1}{2} \left(N - \frac{1}{2} \right) \right] \quad (55)$$

The classical time T_{cl} is defined as:

$$T_{cl} = \frac{2\pi}{\omega_0 (2\bar{I} + 1)}. \quad (56)$$

T_{cl} is the period of a classical rotator having angular momentum $I = \bar{I}$. At times $t = (m/n)T_{rev}$ where $2m < n$ (m and n are mutually prime integers) we will use the trick developed in [1] to write the quadratic exponential in I as

$$e^{-i2\pi I^2 \frac{m}{n}} = \sum_{s=0}^{l-1} a_s e^{-i2\pi I \frac{s}{n}} \quad (57)$$

It is necessary to distinguish three cases:

- a) n is odd, then $l = n$ and all the coefficients a_s are nonzero. However they have the same modulus $1/\sqrt{l}$.

b) n is even and multiple of four, then $l = n/2$ and the modulus of the a_s have the same value as above.

c) n is even and not multiple of four, then $l = n$ but the a_s with even s are zero, the other have their modulus equal to $1/\sqrt{n/2}$.

The number of values of the a_s which are nonzero is called q with $q = n$ if n is odd and $q = n/2$ if n is even. The phase of the a_s can be calculated as said in [1]. Using these results and inserting (55) into (53) one obtains eqs. (58),(59) below:

$$\Psi_\eta(\theta, \phi, \frac{m}{n}T_{rev})_{general} = \sum_I \lambda_I \sum_{s=0}^{l-1} a_s e^{-i2\pi(\frac{m}{n} + \frac{s}{l})} \mathcal{Y}_\eta^I(\theta, \phi) \quad (58)$$

$$= \sum_{s=0}^{l-1} a_s \Psi_{cl}^s(\theta, \phi, t_s) . \quad (59)$$

At times $t = (m/n)T_{rev}$ any WP is a sum of q fractional WP Ψ_{cl}^s each with a different effective time t_s

$$t_s = (\frac{m}{n} + \frac{s}{l})T_{rev} \quad (60)$$

The fractional WP at times t_s is given by

$$\Psi_{cl}^s(\theta, \phi, t_s) = \sum_I \lambda_I e^{-iI\omega_0 t_s} \mathcal{Y}_\eta^I(\theta, \phi) . \quad (61)$$

There are several cases for which all the Ψ_{cl}^s are clones of the initial WP defined by (22) for all possible values of t_s . There are also cases where only one of all the fractional waves is a clone for particular t_s . Let us describe now these events keeping in mind as far as possible arbitrary λ_I .

A. Cloning of circular WP

If $\eta = 1$ one has

$$e^{-iI\omega_0 t_s} \mathcal{Y}_1^I(\theta, \phi) = e^{-iI\omega_0 t_s} Y_I^I(\theta, \phi) = Y_I^I(\theta, \phi - \omega_0 t_s) . \quad (62)$$

Independently of the λ_I the fractional waves verify the cloning property

$$\Psi_{cl}^s(\theta, \phi, t_s) = \Psi(\theta, \phi - \omega_0 t_s, 0) . \quad (63)$$

Among all circular WP which all clone in this way, the exponential WP, which can be sharply localized in the angle θ by considering high enough N , clone accordingly around q directions disposed symmetrically in the Oxy plane defined by q values of the angle $\omega_0 t_s$.

B. Cloning for some particular t_s

This special situation occurs when there exist values of s such that $\omega_0 t_s$ is a multiple of 2π and for which a_s is non zero. Let s_0 be defined by $s_0 = n - m$. One has the property

$$\Psi_{cl}^{s_0}(\theta, \phi, t_{s_0}) = \Psi(\theta, \phi, 0) . \quad (64)$$

This event occurs whenever n is odd or even and not multiple of four. The clone is found always identical to the initial WP. Obviously it is multiplied by a_{s_0} . The existence of the clone is independent of the λ_I and of η . For the values of $s \neq s_0$ the fractional WP are different from the initial WP. Starting from $\eta = 1$ their shape evolve with η and we propose to call them *mutants*. This *mutation* can indeed be seen as a transition between two symmetries as we will show numerically in section V.

C. Symmetry properties of the fractional waves

In the following discussion it will be assumed that $\lambda_I \neq 0$ both for even and odd values of I . If some further symmetry is assumed (for exemple $\lambda_I = 0$ for odd I) new properties will result which will not be discussed in the present paper.

The first remark is that, apart for the value s_0 defined above associated to a clone, the fractional waves can be paired for each value of m and n in the following manner: associated to s there exists an other value s' such that

$$e^{+i I \omega_0 t_{s'}} = e^{-i I \omega_0 t_s} , \quad (65)$$

and also (noting a difference in the sign of η in the right side)

$$\Psi_{cl}^{s'}(\theta, \phi, t_{s'})_{\eta} = \Psi_{cl}^s(\theta, \phi, t_s)_{-\eta}^* . \quad (66)$$

This equation shows that the fractional waves corresponding to opposite η , i.e. opposite $\langle L_z \rangle$, are intermixed. The equality (66) is based on the equality which defines s' in terms of s

$$\frac{t_s + t_{s'}}{T_{rev}} = 0 \pmod{1} \quad (67)$$

from one hand and from the conjugation property

$$\mathcal{Y}_{\eta}^I(\theta, \phi) = \mathcal{Y}_{-\eta}^{I*}(\theta, \phi) . \quad (68)$$

In addition to being real it is important that λ_I should be an even function of η (like for the exponential WP defined by (38-39)).

For $\eta = 0$ the fractional waves Ψ_{cl}^s and $\Psi_{cl}^{s'}$ have the same probability density on the sphere. This leads to a reduction in the number of fractional waves which occur: for odd n there will be one clone plus $(n-1)/2$ fractional waves, for even n and not multiple of four there is one clone and $(n-2)/4$ fractional waves, finally for n multiple of four there will be $n/4$ fractional waves.

V. NUMERICAL CALCULATIONS WITH EXPONENTIAL WP

In this section we will describe some figures showing the time evolution of typical exponential coherent WP. The value of N will generally be the same and we will change the parameter η . Most of the figures are calculated for $N = 20$. This value is typical for a rather concentrated WP. Values near unity correspond to broad WP which occupy the whole of the sphere and are not interesting for our purpose. Let us remind that keeping the same N and changing η produces the same probability density (24) at $t = 0$ however formula (38-39) shows that the distribution of the partial wave depends strongly on η . The average \bar{I} is very low for $\eta = 0$ and this produce a difference in the time evolution which shows less structure if $N = 20$ and if η is decreased. These features can be seen if one study the autocorrelation function represented for three values of η in figure 2. It is seen that this function is composed of peaks which have a larger width if η is small. The structure becomes very rich if η is nearer to 1. This autocorrelation function is very much similar to that studied in ref. [24].

A. Cloning for circular WP

The time evolution of the circular wave packet corresponding to $N = 20$ is shown in Fig. 3 and Fig. 4. In Fig. 3 a convenient set of times have been chosen to show the probability density as a function of θ and ϕ just during the regime of spreading of the wave packet ($t < T_{cl}$) then for a few cloning times followed by the full revival for $t = T_{rev}/2$. In Fig. 4 a "carpet" is shown of the section $0 \leq t \leq T_{rev}/2$ of the probability density for $\theta = \pi/2$ which shows up to $q = 7$ clones.

The difference between Mostowski's coherent state with that created by Atkins and Dobson $|k, s = \frac{1}{2}\rangle_i$ is so tiny that it does not present any interest to be shown. Despite the analogy with the one dimensional results of the infinite square well [2] and the two dimensional rotor [11] some new interesting aspects of our results need to be stressed. Indeed the circular WP spread in a way in the ϕ direction and clone around the Oxy plane, which is natural since there is a linear momentum along Oy initially. However there is no change in time in the azimuthal spread.

The cloning mechanism found in quantum mechanics is not possible for a single classical particle however it will appear if one uses the ensemble interpretation of quantum mechanics as underlined by authors of ref. [4].

B. Linear WP

For $\eta = 0$ the fractional WP has cylindrical symmetry around Ox at all times since it is written as

$$\Psi_{cl}(\theta', \phi', t) = \sum_I b_I e^{-2i\pi I t/T_{rev}} Y_0^I(\theta', \phi'). \quad (69)$$

The quantity $2\pi \sin \theta' |\Psi_{cl}|^2$ is represented in Fig. 5. This shows that the revival wave packets are rings on the sphere and, due to this special topology, do not clone the initial wave function.

The time evolution of $\Psi_0(\theta', \phi', t)$ is represented in Fig. 6. Since the wave packet is in fact one dimensional, the "carpet" representation provides the essential features of the time evolution. However in order to produce a similar richness than for $\eta = 1$ (and a similar expectation value of L^2) we have increased the value of N for $\eta = 0$ to $N = 50$. On a sphere areas of constant probability density could be represented by parallel circles centered on Ox axis. The pattern of the carpet shown in Fig. 6 is very much resemblant to that discussed recently for a special wave packet in one dimensional box in ref. [38]. Indeed there is a superposition of ridges and valleys with simple slopes as a function of t . The interpretation of this effect can be given in similar terms as in [38]. Note that the quantity plotted in Figs. 6 and 5 has the same boundary conditions as the wave packet on the edge of the box. This produces a reflection effect in Fig. 6 totally absent in Fig. 4 since the boundary conditions are different on the circle. Thus for $\eta = 0$ the WP spreads uniformly in all directions defined by the angle ϕ' .

Such a WP is full nonsense for a single classical particle and takes sense only with the ensemble interpretation.

Another interesting linear WP corresponding to $\eta \rightarrow \infty$ but keeping ηN finite is defined as follows:

$$\Psi_{\eta N}(\theta, \phi) = \frac{1}{\sqrt{4\pi}} e^{i\eta N \sin \theta \sin \phi}. \quad (70)$$

It is derived from the harmonic oscillator WP of the appendix by keeping only the term in p_y . This WP has its probability density uniformly distributed over the sphere and obeys the equation

$$L_y \Psi_{\eta N} = 0. \quad (71)$$

It has therefore cylindrical symmetry around Oy and depends on the angle θ'' defined by

$$\cos \theta'' = \sin \theta \sin \phi. \quad (72)$$

Its expansion in spherical harmonics contains now spherical Bessel functions

$$\Psi_{\eta N} = \sum_I \sqrt{2I+1} j_I(\eta N) Y_0^I(\theta'', \phi''). \quad (73)$$

Obviously the fractional waves have also cylindrical symmetry around Oy but there is in addition, for $t = t_{s_0}$, a uniform clone which interferes with all the other fractional waves. The time evolution is shown in Fig. 7 for $\eta N = 20$. For the small values of t , like $t = 1/100 T_{rev}$, the WP is concentrated almost totally on the hemisphere with $y > 0$ with a spike along Oy surrounded by concentric rings. For $t = 1/50 T_{rev}$ the same behaviour occurs but this time on the hemisphere with $y < 0$. For other times both parts of the sphere are covered with rings and the spike also occurs on both sides of the Oy axis. For $t = T_{rev} m/n$ with small m/n a symmetry between the two hemisphere takes place. The existence of the clone can be seen clearly as a small uniform background at times $t = 1/25 T_{rev}$, $t = 1/10 T_{rev}$. There is always a strong interference between the fractional waves which does not allow to make a clear counting even for small values of m/n .

C. Elliptic WP

For the general elliptic wave packet, as deduced from the previous discussion there are no clones, but partial revivals with different topology. Due to the change of symmetry, it is indeed necessary to make a smooth transition between a system of clones located for $\eta = 1$ in the Oxy plane and a system of rings discussed in the previous subsection. In the system of coordinates adopted in subsection II A and corresponding to $\eta = 0$ these rings have Ox as symmetry axis. The transition from the clones for $\eta = 1$ to the rings for $\eta = 0$ is made by developing for η smaller than 1 a system of pairs of crescents perpendicular to the Oxy plane. This transition is clearly visible for particular fractional revival times in Fig. 8. For a very small value of η the upper part and the lower part of one crescent meet the corresponding

parts of a symmetric crescent in order to build up such a ring symmetric around Ox . Again this change of topology of this construction forbids the cloning of all fractional waves. Most of them revive in shapes different from that of the initial wave packet. We propose to call these fractional wave packets mutants. Example of time evolution of wave packet with $\eta = 0.5$ is given in Fig. 9. It is well seen both in Fig. 8 and in Fig. 9 that clones and mutants can occur in the same time. For example for $\eta = \frac{1}{4}$ and $t = \frac{1}{3}T_{rev}$ there is a fractional revival at $\theta = \frac{\pi}{2}$ and $\phi = 0$ with the same shape as the initial wave packet and two crescents which almost close. This situation is similar to that which exists for $\eta = 0$ also for $t = \frac{1}{3}T_{rev}$. For $\eta = \frac{1}{2}$ and $t = \frac{1}{6}T_{rev}$ the two crescents do not form a ring. Among the three fractional waves which are present there are two which are identical to each other but with larger spread in θ . For this value $\eta = \frac{1}{2}$, there are three different topologies for the five fractional waves. In other publications on a different system [30], we had already found the transition from a gaussian three dimensional wave packet to a vortex ring. Refs. [30] were devoted, as well as our previous works, for the time evolution of such coherent waves in the case where the hamiltonian contains a spin orbit interaction in addition to the harmonic oscillator potential. If the spin is oriented along the initial wave packet displacement (Ox axis), the cylindrical symmetry is imposed on the system and preserved during evolution, a vortex rings appear.

The transition between the two shapes of fractional wave packets can be explained by comparing, as a function of η , the spread of the angle θ to the spread of the angle ϕ . If $\eta = 0$ the wave packet has no privileged direction on the sphere. It spreads therefore equally. In the case when $\eta = 1$ the wave packet is peaked near the plane with $\theta = \frac{\pi}{2}$ and the spread in θ is strongly reduced. The spread in ϕ is seen in the scenario of cloning in the plane xOy . For intermediate values of η , there is a competition between the two effects which manifests itself most strongly in the shape of the fractional waves.

For $\eta > 1$ (results not presented) we have observed a strong reduction of the spread in θ . For particular values of (m/n) , some mutants can be peaked with higher amplitude than their neighbours. This is in direct connection to the increase in p_0 which was necessary in the initial wave packet.

D. Final remarks

We can measure the aperture of the probability density of the WP by the solid angle $\Omega = 4\pi/(4N+1)$ corresponding to the cone defined by $\tan(\theta'/2) = 1/2\sqrt{N}$. The time of spreading τ_η of this wave packet of width ΔL_η (33) is of the order of

$$\tau_\eta = \frac{2\pi}{\omega_0} \frac{1}{\Delta L_\eta}. \quad (74)$$

The difference in spreading with η is clearly seen in the autocorrelation functions represented in Fig. 2. We can also define maximum number of fractional wave packets that can be observed knowing that $\tan(\theta'/2) = 1/2\sqrt{N}$ as

$$q_{max} = \frac{\pi}{\arctan(1/2\sqrt{N})}. \quad (75)$$

This number is confirmed by the observation of the 'carpet' of Fig. 4 for $N = 20$ for which we have up to 7 clones. The lifetime τ'_η of a system of q fractional wave packets can be estimated as

$$\omega_0 \tau'_\eta \Delta L_\eta = \frac{2\pi}{q}. \quad (76)$$

Also in Fig. 4 one sees clearly for $q = 2, 3$ the large intervals of time during which clones are observed.

VI. COHERENT STATES FOR A SYMMETRIC TOP

It is natural to enlarge our previous study to rotational coherent states of symmetric tops which contain an additional degree of freedom. There are several possibilities in the literature for constructing such a state. Our aim is again to choose the axis of coordinates in order to eliminate irrelevant parameters and to make evolution understandable. This is possible only in the case of symmetric top. We will assume that the moments of inertia in the intrinsic frame $J_x = J_y$ and introduce the parameter δ such that:

$$\delta = \frac{J_x}{J_z} - 1. \quad (77)$$

The energy spectrum is then:

$$E(I, K) = \frac{\hbar^2}{2J_x} [I(I+1) + \delta K^2]. \quad (78)$$

A convenient rotational wave packet was defined and studied by Janssen [28] on the basis of the work of Perelomov [36] and Schwinger [27]. This wave packet denoted by three complex numbers x, y and z is a mixture of D_{MK}^I functions

$$\begin{aligned} |xyz\rangle &= \exp\left(-\frac{1}{2}yy^*(1+xx^*)(1+zz^*)\right) \\ &\times \sum_{IMK} \sqrt{\frac{(2I)!}{(I+M)!(I-M)!(I+K)!(I-K)!}} x^{I+M} y^{2I} z^{I+K} |IMK\rangle. \end{aligned} \quad (79)$$

The sum over I contains integer as well as half integer values of I i.e. this state extends that presented by Atkins and Dobson. On a similar line as in section III we call $|xyz\rangle_i$ its normalized projection onto the space with integer I . A particularly convenient choice of x, y and z as well as of the system of coordinates decreases the number of parameters to two and reduces the summation to I and K only. The simpler wave packet is then:

$$|r, \lambda\rangle = \exp(-r) \sum_{IK} (-1)^{I+K} (2r)^I \frac{(\sin \frac{\lambda}{2})^{I+K} (\cos \frac{\lambda}{2})^{I-K}}{\sqrt{(I+K)!(I-K)!}} |I- IK\rangle. \quad (80)$$

If L_X, L_Y, L_Z are the components of \vec{L} in the intrinsic axes, L_x, L_y, L_z those related to the laboratory axes, one has according to Janssen:

$$\langle r\lambda|L_x|r\lambda\rangle = \langle r\lambda|L_y|r\lambda\rangle = 0, \quad \langle r\lambda|L_z|r\lambda\rangle = -r, \quad (81)$$

$$\langle r\lambda|L_Z|r\lambda\rangle = -r \cos \lambda, \quad \langle r\lambda|L_X|r\lambda\rangle = -r \sin \lambda, \quad \langle r\lambda|L_Y|r\lambda\rangle = 0, \quad (82)$$

$$\langle r\lambda|L^2|r\lambda\rangle = r\left(r + \frac{3}{2}\right). \quad (83)$$

Since the WP given by (80) contains only components with $M = -I$ it is a circular WP with $\eta = -1$ which fulfills eq. (2) with the components of \vec{L} taken in the laboratory system. From Janssen's work the components in the rigid body system verify the equation

$$\Delta L_X^2 = \Delta L_Y^2, \quad (84)$$

while their product takes the value

$$\Delta L_X^2 \Delta L_Y^2 = \frac{\langle L_Z \rangle^2}{4 \cos^2 \lambda}. \quad (85)$$

Therefore eq. (2) is also verified for the components in the rigid body system if OZ is directed along \vec{L} . On the other hand the expansion (80) of the rotational coherent states in terms of $|I- IK\rangle$ has the same coefficients as the expansion of Atkins–Dobson in terms of angular momentum eigenstates $|IK\rangle$. The two expansions are connected by defining α_+ and α_- as:

$$\alpha_+ = \sqrt{2r} \sin \frac{\lambda}{2}, \quad \alpha_- = \sqrt{2r} \cos \frac{\lambda}{2}. \quad (86)$$

The projection $|r, \lambda\rangle_i$ deduced by restricting (80) to integer values of I and K verify eqs. (81) to (83) only approximately. However if r is large enough, these equations are obtained in a very good approximation. The time evolution of the wave packet $|r, \lambda\rangle_i$ will be studied in the next section for a rigid body symmetric rotor.

VII. TIME EVOLUTION OF JANSSEN'S COHERENT STATE

The energy spectrum of the axially symmetric rigid rotor is written as:

$$E_{IK} = \hbar\omega_0 [I(I+1) + \delta K^2]. \quad (87)$$

We will study the time evolution of a wave packet deduced from (80) with $\omega_0 = \hbar/(2J_x)$ and with average values

$$\langle r\lambda | L_Z | r\lambda \rangle = \bar{K} \simeq -r \cos \lambda \quad (88)$$

$$\langle r\lambda | L_z | r\lambda \rangle = \bar{I} \simeq -r. \quad (89)$$

The energy E_{IK} is written by taking \bar{K} and \bar{I} as reference, and defining k_1 and k_2 as:

$$k_1 = I - \bar{I} \quad k_2 = K - \bar{K}. \quad (90)$$

$$E_{k_1 k_2} = \hbar\omega_0 [\bar{I}(\bar{I}+1) + \delta\bar{K}^2] + \hbar\omega_0 (2\bar{I}+1)k_1 + \hbar\omega_0 \delta(2\bar{K})k_2 + \hbar\omega_0 k_1^2 + \hbar\omega_0 \delta k_2^2. \quad (91)$$

We now follow the lines drawn by Bluhm, Kostelecky and Tudose [10] who have considered the time evolution of a system which depends quadratically on two quantum numbers, in our case I and K . There are 4 time constants; the first pair defined as

$$T_{cl}^I = \frac{2\pi}{\omega_0(2\bar{I}+1)} \quad T_{rev}^I = \frac{2\pi}{\omega_0} = (2\bar{I}+1) T_{cl}^I \quad (92)$$

is related to the motion around Oz axis (laboratory axis), i.e. it is connected to the Euler angle α , the second pair plays a parallel role, it concerns the motion around the symmetric OZ axis and the Euler angle γ

$$T_{cl}^K = \frac{2\pi}{\omega_0 \delta 2\bar{K}} = \frac{1}{\delta} \frac{2\bar{I}+1}{2\bar{K}} T_{cl}^I \quad T_{rev}^K = \frac{2\pi}{\delta \omega_0} = \frac{1}{\delta} T_{rev}^I. \quad (93)$$

The system of coordinates and the parametrization in (80) enables to profit by the separation of variables in the state $|I - IK\rangle$ since:

$$\langle \alpha\beta\gamma | I - IK \rangle = e^{i\alpha I} d_{-IK}^I(\beta) e^{-i\gamma K} = D_{-IK}^I(\alpha, \beta, \gamma). \quad (94)$$

The wave packet (80) at time t with conditions (88) and (89) and integer I and K will be denoted as $|\bar{I} \bar{K}\rangle$ and written as:

$$\langle \alpha\beta\gamma | \bar{I} \bar{K} \rangle_t = \sum_{IK} C_{IK}(r, \lambda) d_{-IK}^I(\beta) e^{i[\alpha I - 2\pi I(I+1)t/T_{rev}^I]} e^{-i(\gamma K + 2\pi K^2 t/T_{rev}^K)} \quad (95)$$

$$= e^{-i[\bar{I}(\bar{I}+1) + \delta\bar{K}^2]t/T_{rev}^I} \sum_{k_1 k_2} C_{k_1 k_2}(r, \lambda) d_{k_1 k_2}^I(\beta) \quad (96)$$

$$\times e^{i[\alpha k_1 - 2\pi(k_1/T_{cl}^I + k_1^2/T_{rev}^I)t]} e^{-i[\gamma k_2 + 2\pi(k_2/T_{cl}^K + k_2^2/T_{rev}^K)t]}.$$

The summation on I and K has been changed to a sum over k_1 and k_2 and the coefficient $C_{IK} d_{-IK}^I$ has been given the new indexes. The discussion of the time evolution of (95-96) follows in a straightforward manner that given by Bluhm, Kostelecky and Tudose [10]. The crucial parameter is δ . If T_{rev}^K and T_{rev}^I are not commensurate there is no cloning, however for $t = (m/n)T_{rev}^I$ there are partial revivals in the variable α : i.e. the wave packet is a superposition of q fractional wave packets peaked regularly along the Oz axis. ($q = (n/2)$ if n is even, n in other cases). For $t = (m'/n')T_{rev}^K$ the same scenario of partial revival occurs but this time there are q' fractional wave packets peaked around the OZ axis. [$q' = (n'/2)$ if n' is even, n' otherwise].

The interesting situation of commensurability of T_{rev}^I and T_{rev}^K allows, on the contrary, the construction of q^2 clones for all the time such that

$$t = \frac{m}{n} T_{rev}^{I,K} \quad (97)$$

The revival time $T_{rev}^{I,K}$ is the least common multiple of T_{rev}^I and T_{rev}^K

$$p T_{rev}^I = r T_{rev}^K = T_{rev}^{I,K}. \quad (98)$$

The time evolution of the rotational wave packets is presented in Fig. 10 and Fig. 11.

The particular choice $\bar{K} = 0$ leads to $T_{cl}^K = \infty$ but T_{rev}^K is finite as well as T_{cl}^I and T_{rev}^I . For the smaller value of t , the behaviour of the wave packet around Oz and OZ is different as seen from Fig. 11. There is indeed a classical rotation and spreading around Oz while no rotation occurs around OZ , only the spreading is observed around this axis.

Fig. 10 illustrates the case of an irrational value of δ where there are partial revivals for times $t = (m/n)T_{rev}^I$ around Oz and for times $t = (m'/n')T_{rev}^K$ where the revivals are around OZ . Note that the concentration of the wave packet for some definite values of α (or γ) has no influence on the other variable γ (or α) respectively.

Fig. 11 illustrates the case of a rational value of δ , for which there are q^2 clones. The proof that there are q^2 clones if condition (98) holds is rather simple, one applies twice the method of Averbukh and Perelman to linearize the exponential containing k_1^2 and k_2^2 in eq. (95-96).

Finally we want to stress that the variable β does not play a role in the time evolution. Obviously this is due to our particular choice of axis in eq. (80). The role played by β for the axial rotor is similar to the role played by θ in the diatomic molecule.

VIII. CONCLUSIONS

We have discussed the time evolution of angular momentum coherent states that are built from intelligent spin states, but as pointed in the Appendix, can be constructed by a simple, purely geometric, generating procedure. The basic ingredients are the three dimensional gaussian wave packets of the harmonic oscillator. We have used two of the parameters of the gaussian to derive an ensemble of coherent states which depend finally on two parameters N and η . The angular distribution of the probability density depends only on N , while the momentum distribution depends both on N and η . The uncertainty relation (2) is valid for all N and η . Such a variety of wave packets do not arise from the previous works on angular momentum coherent states with bosons. It is for example simple to show [32] that there is no place in the Atkins and Dobson or Mihailov's work for the wave packets (40-41) which correspond to $\eta = 0$. Also the coefficient α_{jm} defined by (45) in terms of α_+ and α_- cannot be put generally in the form such that (44) which ensures that b_{IM} is zero if I and M have an opposite parity.

In the framework of the scenario of ref. [1] we have shown that for $\eta = 1$ the wave packets spread at $t = \frac{m}{n}T_{rev}$ into clones. However, the difference between the symmetries for $\eta = 0$ and $\eta = 1$ necessitates a change in the topology of the fractional wave packets. This change is such that these wave packets can be named mutants after a certain amount of deformation of their shape. Aronstein and Stroud [2] have shown "that, the infinite square well is an ideal system for fractional revivals since all wave functions exhibit fractional revivals of all orders". The same statement applies to the case of the diatomic molecule but is limited however to circular wave packets, i.e. to those which contain only $M = I$ partial waves in a convenient system of axis. The generation mechanism used in this paper can be extended to shapes different from gaussian distribution. Clones will always result in this particular condition. For the wave packets which contain populations of sublevels $M \neq I$, mutants will appear. All these results hold independently on the realization of the uncertainty condition (2). For systems where energy is quadratic in one quantum number we have shown that the time evolution can exhibit a rich structure of cloning and mutation of fractional revivals. It is a challenging question to find a proper way to excite such wave packets in a rotational band of a molecule or of a deformed nucleus. Let us briefly describe the efforts made under this perspective.

The wave packets with $\eta = 0$ or wave packets with $M = 0$ have been already considered several times. In a reference work on Coulomb excitation of nuclei with heavy ions R.A. Broglia and A. Winther [31] have shown that such wave packets are generated in backward scattering. Their population of the excited states of a rotational band with $K = 0$ do not coincide with the very simplified expression (40-41). Indeed interference effects during the excitation process modulates this population to a large extent (Fig. 8, p.82 of ref. [31]). However, we have studied the time evolution of such a wave packet and this will be the subject of a future publication [40].

The authors of ref. [32] have written an important analysis on coherent rotational states, completing the work of [31]. They have already used the wave $|k, \frac{1}{2}\rangle_i$ of section III derived from [26], and they have also considered an extension toward other symmetries like $Sp(2,R)$, $Sp(4,R)$. Time evolution was studied but only for the average values of operators like quadrupole moments. The physical systems considered were the nucleus ^{238}U and the molecule CS_2 . The time evolution of expectation values of more general operators for wave packets due to quadratic dependence was studied in [37]. The operators studied in ref. [32] have very strict selection rules and the time evolution reflected there is much poorer than what is exhibited by the full wave packet and by the average values of the more complex observables [37] related to the position. It is, however, clear that all the wave packets considered in ref. [32] must evolve according to the scenario of ref. [1] with a very rich sequence of changes of shapes.

Our work comes very near from the spirit of two recent publications devoted to molecular physics. In ref. [39] the

population of a set of rotational states of a molecule by an intense laser has been calculated. However, the number of states excited in this way is rather small, $l < 4$, the symmetry implies only states with $M = 0$ and therefore the WP produced is not concentrated on the sphere as sharply as ours with $N = 20$ or 50. In ref. [41] Ortigoso has studied how to tailor microwaves pulses in order to create rotational coherent states for an asymmetric-top molecule, which are built from Radcliffe's intelligent spin states discussed in section II. It is gratifying that such a mechanism which involves optimal control theory is possible. However our demand is more ambitious since one needs to combine intelligent spin states of different angular momentum in order to achieve a proper angular concentration. In addition one has to find a mechanism that allows to change continuously our variable η , i.e. the relative uncertainties in L_x and L_y , in order to explore the whole variety of our states as well as of the intelligent spin states. It is indeed interesting that Radcliffe's states have been used quite thoroughly for example in ref. [42,43] but our paper points toward the fact that a richer structure exists nearby in accordance to older works [19–21]. As said in the text we have not used the larger class of intelligent spin states in the case of the diatomic molecule and we are also conscious that our work on the symmetric top leaves open possibilities of coherent states that have not yet been explored.

It is worth to mention very recent paper by Chen and Yeazell [44] on an analytical wave packet design scheme that is able to create desired Rydberg wave packets and control their dynamics.

We believe that we have enriched anyway the examples given in the reference [10] by pointing out how different the fractional revivals may be.

APPENDIX A: CONNECTION BETWEEN THE EXPONENTIAL COHERENT WP AND COHERENT STATES OF THE HARMONIC OSCILLATOR

The exponential WP defined by eq. (23) can be manufactured from gaussian wave packets in three dimensions which are coherent states of the harmonic oscillator. Such a general WP with an average position \vec{r}_0 and momentum \vec{p}_0 are written as

$$\Psi_G(r, \theta, \phi) = \frac{1}{(2\pi)^{\frac{3}{4}} \sigma^{\frac{3}{2}}} \exp \left[-\frac{(\vec{r} - \vec{r}_0)^2}{2\sigma^2} + i \frac{\vec{p}_0 \cdot \vec{r}}{\hbar} \right]. \quad (\text{A1})$$

One gets rid of three unnecessary parameters if one chooses the axis in such a way that

$$p_{0z} = 0, \quad \vec{r}_0 = \hat{x} r_0. \quad (\text{A2})$$

With such choices the probability density is

$$|\Psi_G|^2 = \left[\frac{1}{(2\pi)^{3/2} \sigma^3} \exp \left(-\frac{r^2 + r_0^2}{\sigma^2} \right) \right] \exp \left(\frac{2r r_0}{\sigma^2} \sin \theta \cos \phi \right). \quad (\text{A3})$$

Apart from a normalization factor it coincides with eq. (24) if r and r_0 are both chosen as

$$r = r_0 = \sigma \sqrt{N}. \quad (\text{A4})$$

The solid angle $\Omega = 4\pi/(4N + 1)$ is thus the angle with which the width σ of the density of the gaussian WP is observed from the center of the sphere of radius given by (A4). This choice still leaves two parameters p_{0x} and p_{0y} free. The choice which leads to (23) is

$$p_{0x} = 0, \quad r_0 p_{0y} = \eta N \hbar. \quad (\text{A5})$$

If one takes the width of the harmonic oscillator $\sigma = \sqrt{\hbar/m\omega}$ the value of p_{0y} given in (A5) leads for $\eta = 1$ to

$$p_{0y} = m r_0 \omega. \quad (\text{A6})$$

The coherent state (A1) associated to this value evolves around a circular trajectory in the field of the harmonic oscillator. In the same manner the value $\eta = 0$ is associated to a linear trajectory and the other values of η correspond to elliptic trajectories. In the second case the initial point is either the apogee or the perigee of the ellipsis. In this manner more general WP can also be constructed which start from arbitrary points according to a nonzero value given to p_{x0} . Let us define a parameter ϵ by

$$r_0 p_{0x} = \epsilon N \hbar. \quad (\text{A7})$$

The exponential WP (23) becomes in these new conditions

$$\Psi_{\eta,\epsilon}(\theta, \phi) = \sqrt{\frac{N}{2\pi \sinh 2N}} e^{N \sin \theta [(1+i\epsilon) \cos \phi + i\eta \sin \phi]} \quad (\text{A8})$$

and verify the condition

$$[(1+i\epsilon)L_x + i\eta L_y] \Psi_{\eta,\epsilon} = 0. \quad (\text{A9})$$

The probability density is again given by (24). However these more general states do not fulfill condition (2). Indeed for those states which obey this equation there exists a value of η given by (7) such that eq. (6) is obeyed and eq. (A9) is not. It was then consistent to consider only those WP with $\epsilon = 0$. This result is in accordance with an older result by Rashid [21] and mark a difference between so called *quasi-intelligent spin states* which solve (A8) but not satisfy (2) and the *intelligent spin states* for which $\epsilon = 0$.

* E-mail: arvieu@isn.in2p3.fr

† E-mail: rozmej@tytan.umcs.lublin.pl and rozmej@isnhp1.in2p3.fr, <http://tytan.umcs.lublin.pl/users/rozmej/index.html>

- [1] I.S. Averbukh and N.F. Perelman, Phys. Lett. A **139** 449 (1989);
I.S. Averbukh and N.F. Perelman, Usp. Fiz. Nauk. **161** 41 (1991); [Sov. Phys. Usp. **34**(7) 572 (1991)].
- [2] D.L. Aronstein and C.R. Stroud Jr., Phys. Rev. A **55** 4526 (1997).
- [3] Z. Dačić-Gaeta and C.R. Stroud, Jr., Phys. Rev. A **42** 6308 (1990);
J.C. Gay, D. Delande and A. Bommier, Phys. Rev. A **39** 6587 (1989);
M. Nauenberg, Phys. Rev. A **40**, 1133 (1989).
- [4] M. Nauenberg, C.R. Stroud, Jr. and J.A. Yeazell, Scientific American, June 1994, 24.
- [5] S.D. Boris, S. Brandt, H.D. Dahmen, T. Strohm, and M.L. Larsen, Phys. Rev. A **48** 2574 (1993).
- [6] R. Bluhm and V.A. Kostelecky, Phys. Rev. A **51** 4767 (1995).
- [7] C. Leichtle, I.Sh. Averbukh and W.P. Schleich, Phys. Rev. Lett. **77** 3999 (1996);
C. Leichtle, I.Sh. Averbukh and W.P. Schleich, Phys. Rev. A **54** 5299 (1996).
- [8] R.M. Bowman, M. Dantus and A.H. Zewail, Chem. Phys. Lett. **161** 297 (1989).
- [9] M.J.J. Vrakking, D.M. Villeneuve and A. Stolow, Phys. Rev. A **54** R37 (1996).
- [10] R. Bluhm, V.A. Kostelecky and B. Tudose, Phys. Lett. A **222** 220 (1996).
- [11] R. Bluhm, V.A. Kostelecky and J.A. Porter, Am. J. Phys. **64** 944 (1996).
- [12] G. Alber and P. Zoller, Phys. Rep. **199** 231 (1991);
B.M. Garraway and K.A. Suominen, Rep. Prog. Phys. **58** 365 (1995).
- [13] M.V. Berry and J. Goldberg, Nonlinearity **1** 1 (1988).
- [14] M.V. Berry, Physica D **33** 26 (1988).
- [15] M.V. Berry and S. Klein, J. Mod. Opt. **43** 2139 (1996).
- [16] M.V. Berry J.Phys. A **29** 6617 (1996).
- [17] J.R. Klauder and B.S. Skagerstam, *Coherent States*, (World Scientific, Singapore (1985)).
- [18] F. Bloch, Phys. Rev. **70** 460 (1946).
J.M. Radcliffe, J. Phys. A **4** 313 (1971).
- [19] C. Aragone, G. Guerri, S. Salamo and J.L. Tani, J. Phys. A **7** L149 (1974).
- [20] C. Aragone, E. Chalbaud and S. Salamo, J. Math. Phys. **4** **17** 1963 (1976).
- [21] M.A. Rashid, J. Math. Phys. **19** 1391 (1976); **19** 1397 (1976).
- [22] L. Kolodziejczyk and A. Ryter, J. Phys. A **7** 213 (1974).
- [23] G. Vetri, J. Phys. A **8** L55 (1975).
- [24] S.I. Vetchinkin, A.S. Vetchinkin, V.V. Eryomin and I.M. Umanskii, Chem. Phys. Lett. **215** 11 (1993).
- [25] J. Mostowski, Phys. Lett. A **56** 369 (1976).
- [26] P.W. Atkins and J.C. Dobson, Proc. Roy. Soc. Lond. A **321** 321 (1971).
- [27] J. Schwinger, in: *Quantum Theory of Angular Momentum*, L.C. Biedenharn and H. van Dam (eds.), Academic Press, New York (1965).
- [28] D. Janssen, Yad. Fiz. **25** 897 (1977), [Sov. J. Nucl. Phys. **25** 479 (1977)].
- [29] R. Jackiw, J. Math. Phys. **9** 339 (1968).
- [30] R. Arvieu and P. Rozmej, Phys. Rev. A **51** 104 (1995);
R. Arvieu, P. Rozmej and W. Berej, J. Phys. A **30** 5381 (1997).

- [31] R. Broglia and A. Winther, *Heavy Ion Reactions*, (Benjamin, New York (1981)).
- [32] L. Fonda, N. Mankoč-Borstnik and M. Rosina, Phys. Rep. **158** 159 (1988).
- [33] R. Bonifacio, D.M. Kim and M.O. Scully, Phys. Rev. **187** 441 (1969).
- [34] V.V. Mikhailov, Theor. Math. Phys. **15** 584 (1973); Phys. Lett. A **34** 343 (1971).
- [35] P. Gulshani, Can. J. Phys. **57** 998 (1979); **25** 479 (1977).
- [36] A.M. Perelomov, Commun. Math. Phys. **26** 222 (1972).
- [37] P.A. Braun and V.I. Savichev, Phys. Rev. A **49** 1704 (1994).
- [38] F. Grossmann, J.M. Rost and W.P. Schleich, J. Phys. A **30** L277 (1997).
- [39] M. Persico and P. Van Leuven, Z. Phys. D **41** 139 (1997).
- [40] R. Arvieu and P. Rozmej, (to be published).
- [41] J. Ortigoso, Phys. Rev. A **57** 4592 (1998).
- [42] D. Huber, E.J. Heller and W.G. Harter J. Chem. Phys. **87** 1116 (1987).
- [43] C.C. Martens J. Chem. Phys. **96** 1870 (1992).
- [44] X. Chen and J.A. Yeazell, Phys. Rev. A **57** R2274 (1998).

FIG. 1. Probabilities to find the partial waves Y_l^J in the coherent states of Mostowski (solid line) and Atkins–Dobson (dashed impulses) for parameters $N = 20 = 1/2(k^2 + 1)$ ensuring the same angular velocity for both wave packets.

FIG. 2. The autocorrelation function for $N = 20$ and different values of parameter η corresponding to a smooth transition between two different symmetries.

FIG. 3. Time evolution of Mostowski’s wave packet with $N = 20$. The left column represents changes of the probability density during short term evolution, the right one at fractional revival times. The probability density at times equal $1/5$, $1/3$ and $1/2 * T_{rev}$ are identical with those presented at $1/10$, $1/6$ and $n * T_{rev}$, respectively. (The vertical scale is not the same in all figures.)

FIG. 4. Time evolution of Mostowski’s wave packet with $N = 20$. The $|\Psi_M(\theta, \phi, t)|^2$ for fixed $\theta = \pi/2$ is presented in the contour plot. The larger values of $|\Psi_M(\theta, \phi, t)|^2$ result in heavy lines due to almost overlapping cuts for fractional revivals. One can clearly see the fractional revivals of orders $1/7$, $1/12$, $1/5$, $1/8$, $1/6$, $1/4$ and so on (corresponding times are $1/7$, $1/6$, $1/5$, $1/4$, $1/3$ and $1/2$ of T_{rev}).

FIG. 5. Time evolution of the Ψ_{cl} (69) for $N = 50$. The probability density $2\pi \sin \theta' |\Psi_{cl}|^2$ is presented as a function of θ' and t within one revival period.

FIG. 6. Time evolution of the wave packet (35-36) for $N = 50$. The probability density $2\pi \sin \theta' |\Psi|^2$ is presented in the contour plot. The larger values of $2\pi \sin \theta' |\Psi|^2$ result in heavy lines due to almost overlapping cuts for fractional revivals.

FIG. 7. Time evolution of the WP (70) with infinite η but $\eta N = 20$. At $t = 0$ the probability density is $1/4\pi$. See explanations in the text.

FIG. 8. Transition of fractional wave packets from exact clones ($\eta = 1$) through developing crescents ($\eta = 1/2, \eta = 1/4$) to ring topology ($\eta = 0$) is demonstrated for two fractional revival times $t = 1/3 * T_{rev}$ (left) and $t = 1/4 * T_{rev}$ (right). The fractional waves called mutants are clearly seen in the lower rows of the figure.

FIG. 9. Time evolution of the coherent state deduced from elliptic motion ($\eta = 0.5$). The time sequence presented here is the same as in Fig. 3. Comparing to this figure the crescents are clearly visible, they are the most pronounced for $t = \frac{1}{4} T_{rev}$.

FIG. 10. Time evolution of Janssen’s coherent state for axially symmetric top (95-96) for irrational $\delta = 1/\sqrt{3}$ implying $T_{rev}^I = 1/\sqrt{3} T_{rev}^K \simeq 0.577 T_{rev}^K$. Shown is the probability density $|\langle \alpha \beta \gamma | \bar{I} \bar{K} \rangle|^2$ for $\beta = \pi/2$, $\bar{I} = 4$ and $\bar{K} = 0$. Notice that the vertical scale is not the same in all figures.

FIG. 11. The same as in Fig. 10 but for rational $\delta = 1/2$ implying $T_{rev}^{I,K} = T_{rev}^K = 2 T_{rev}^I$. Clones for times $1/6$, $1/3$ and $1/2 T_{rev}^{I,K}$ are clearly visible as well as full revivals. Notice that the vertical scale is not the same in all figures.

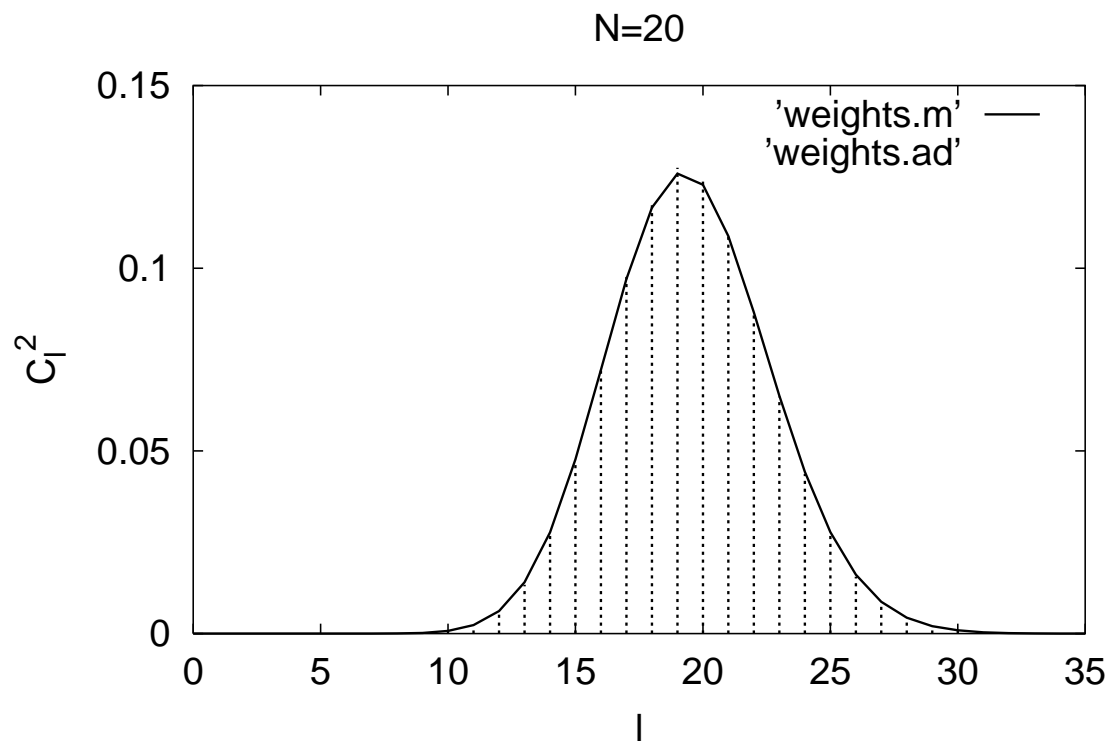


FIG. 1. Probabilities to find the partial waves Y_l^j in the coherent states of Mostowski (solid line) and Atkins–Dobson (dashed impulses) for parameters $N = 20 = 1/2(k^2 + 1)$ ensuring the same angular velocity for both wave packets.

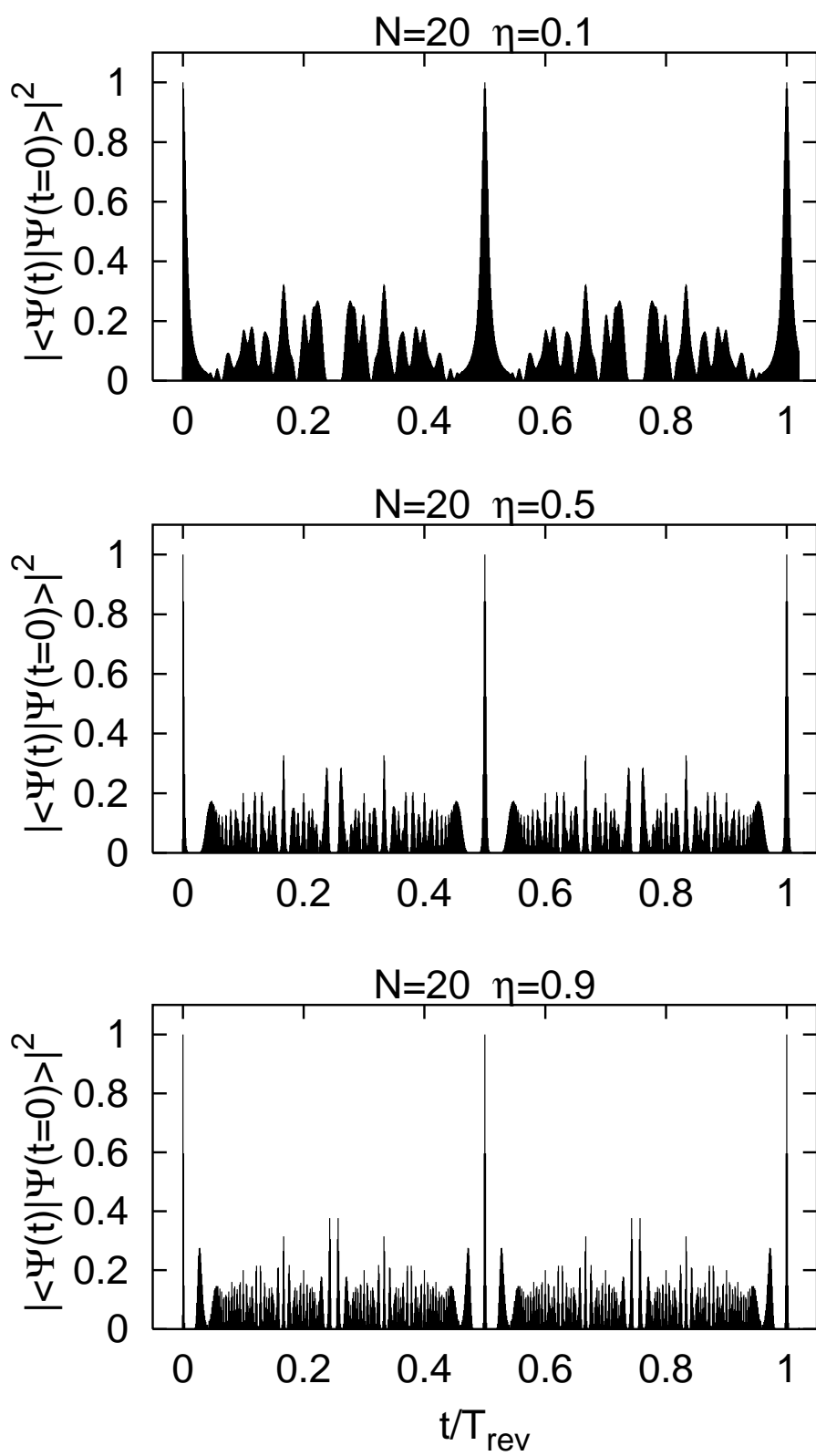
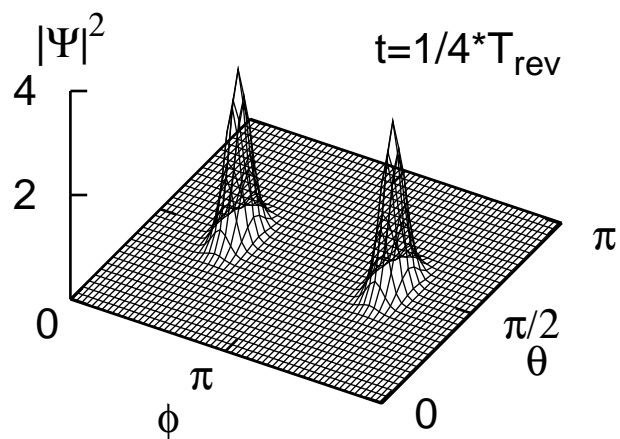
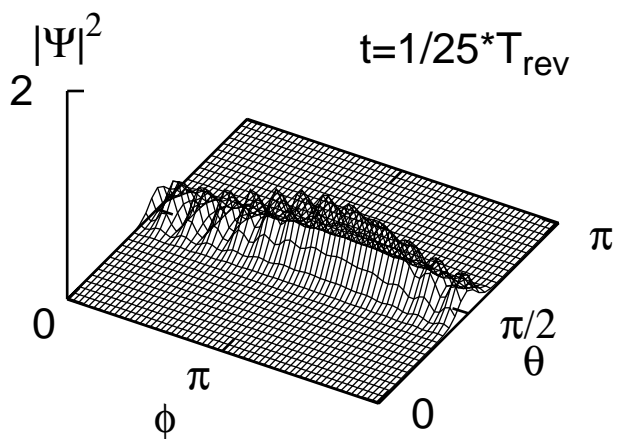
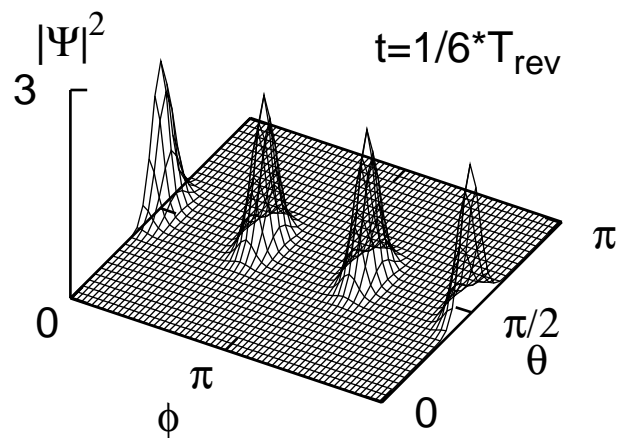
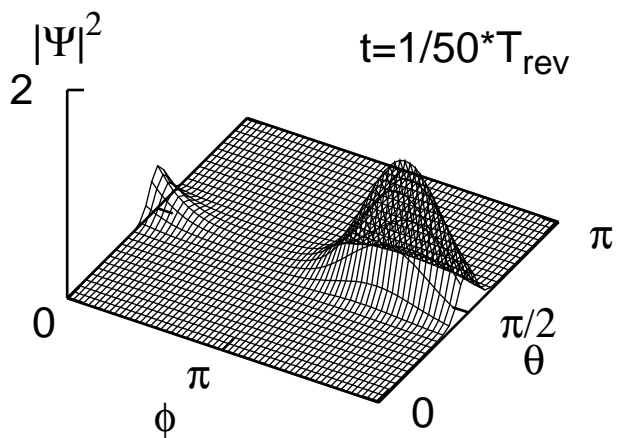
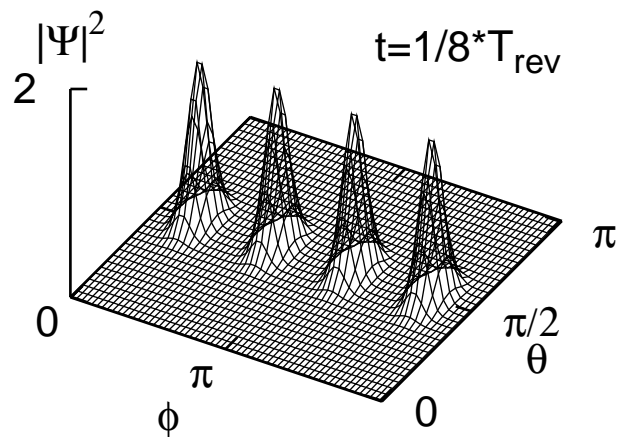
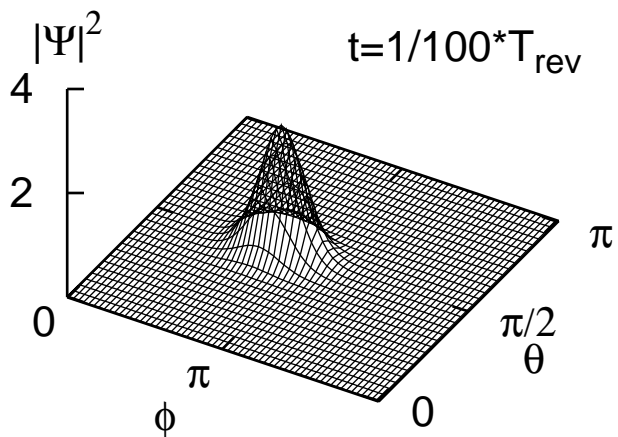
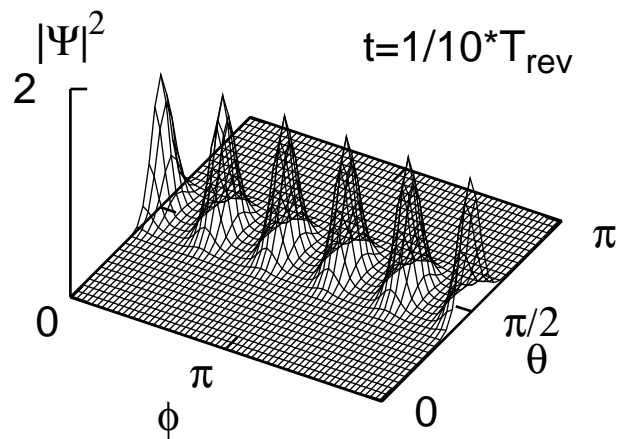
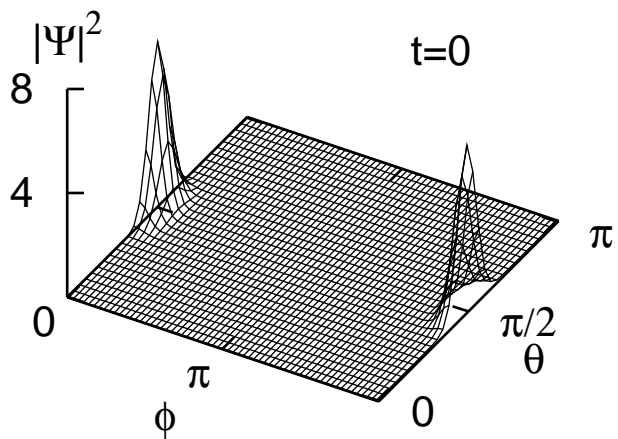
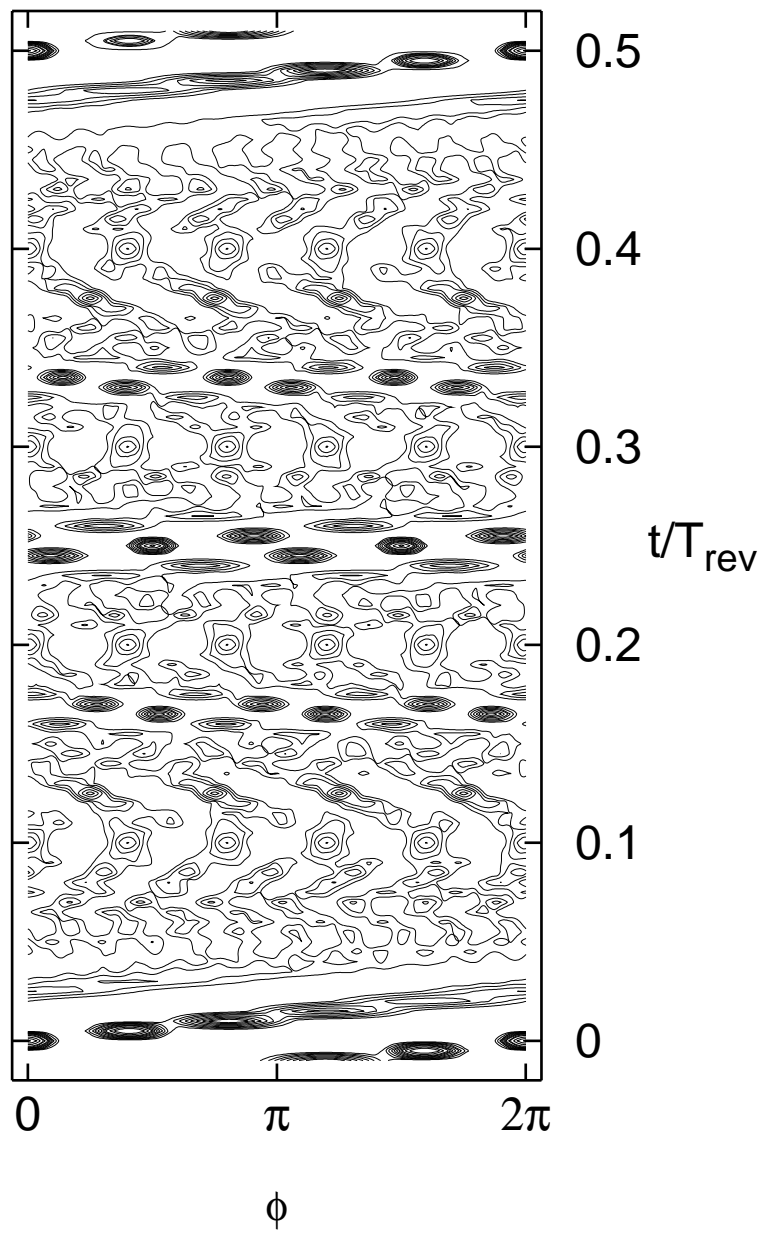


FIG. 2. The autocorrelation function for $N = 20$ and different values of parameter η corresponding to a smooth transition between two different symmetries.

N=20 $\eta=1$



$N=20 \quad \eta=1$



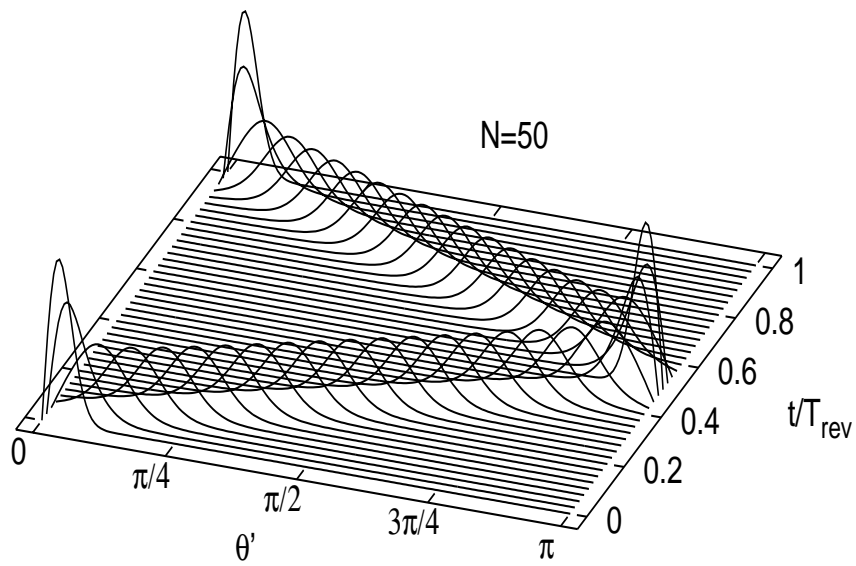
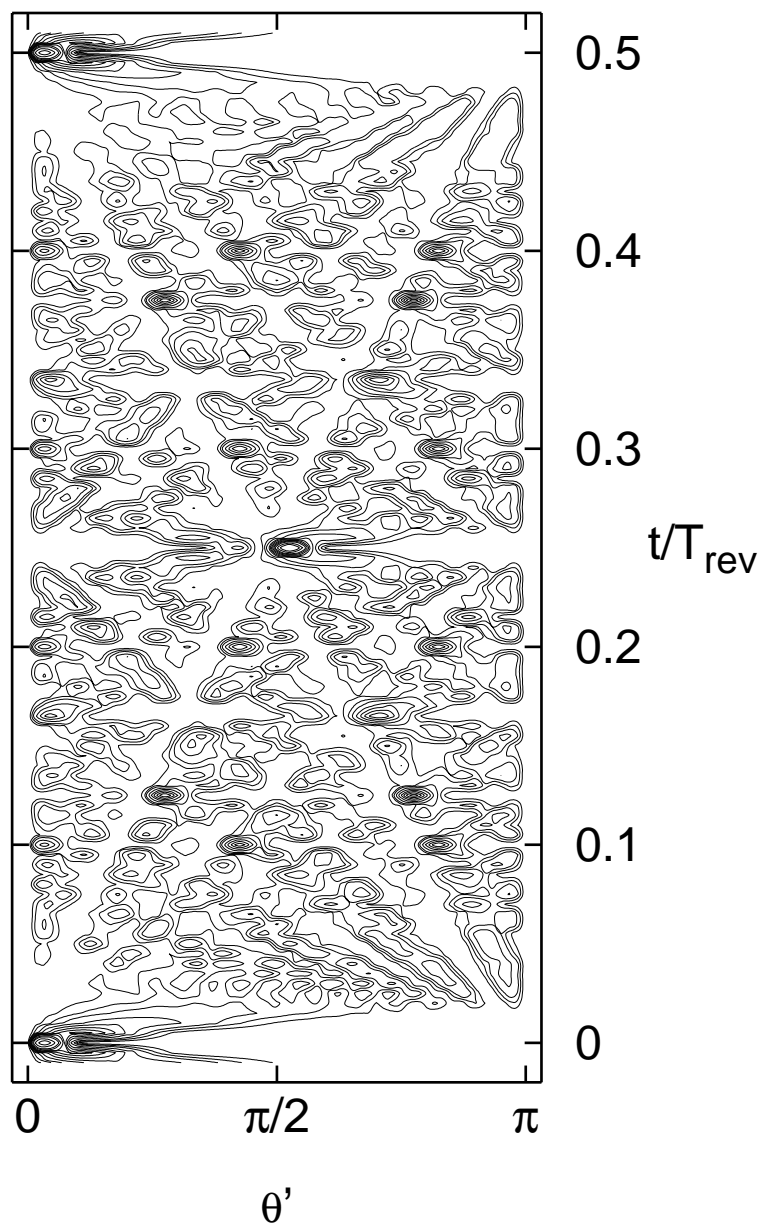
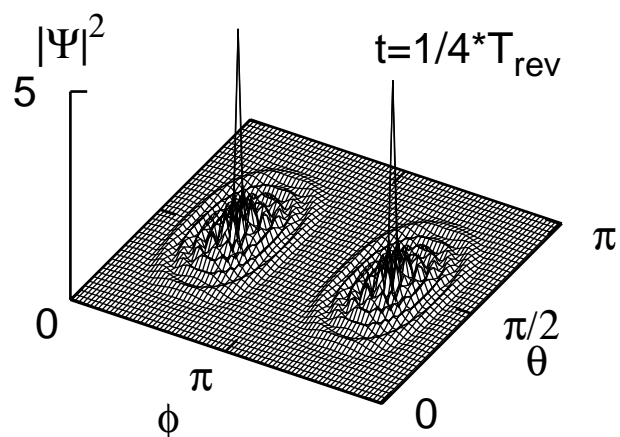
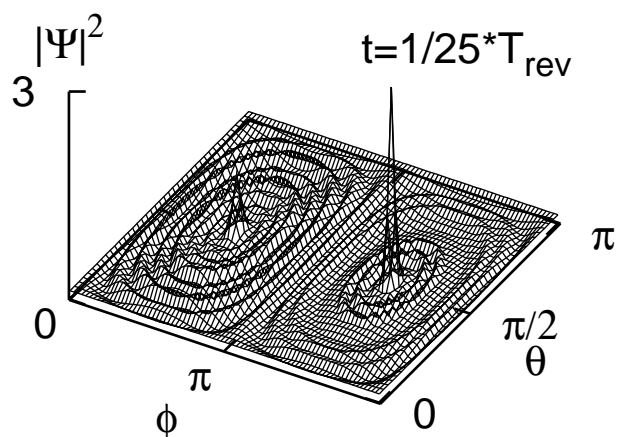
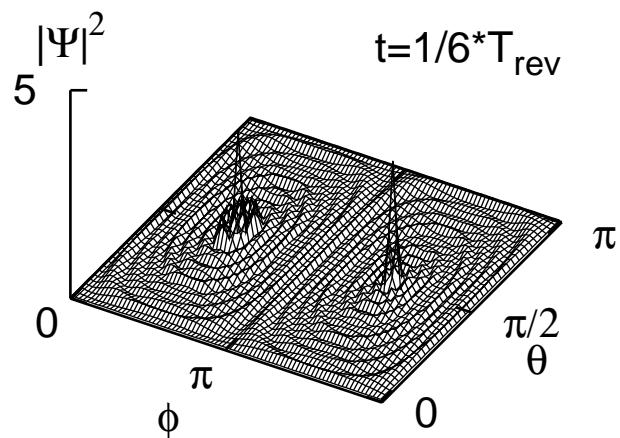
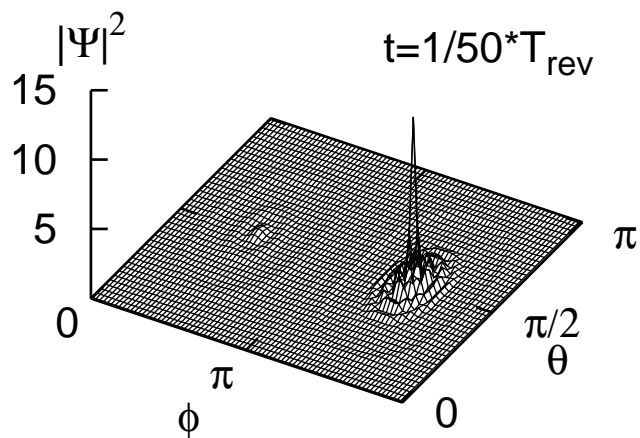
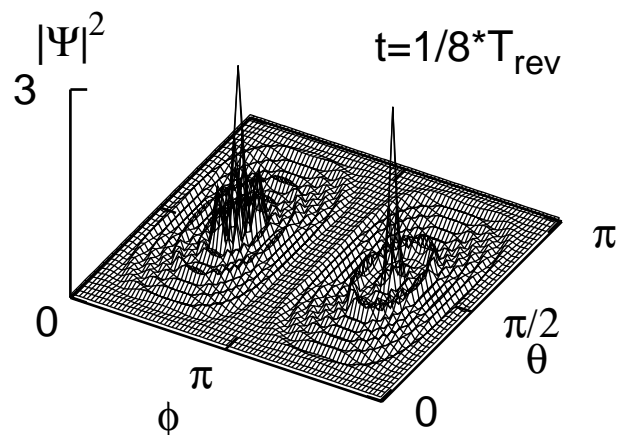
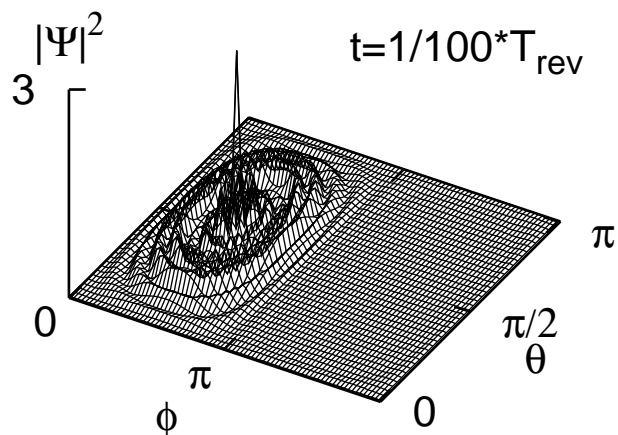
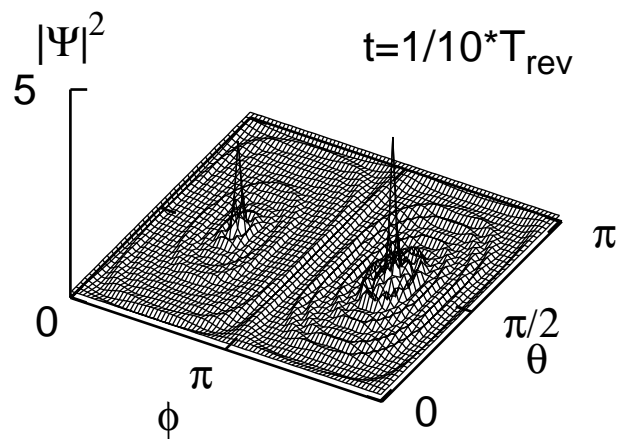
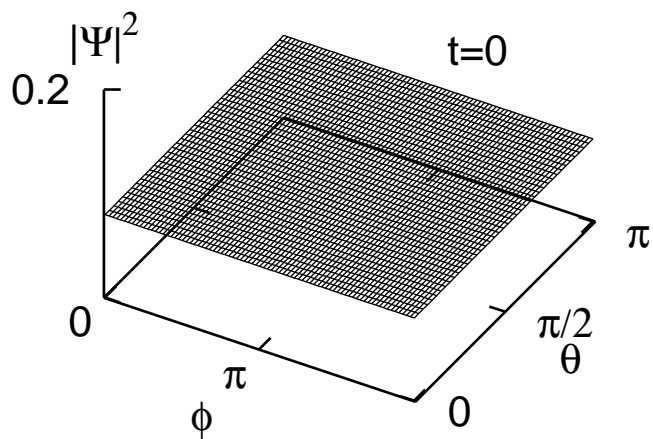


FIG. 5. Time evolution of the Ψ_{cl} (69) for $N = 50$. The probability density $2\pi \sin \theta' |\Psi_{cl}|^2$ is presented as a function of θ' and t within one revival period.

$N=50 \quad \eta=0$



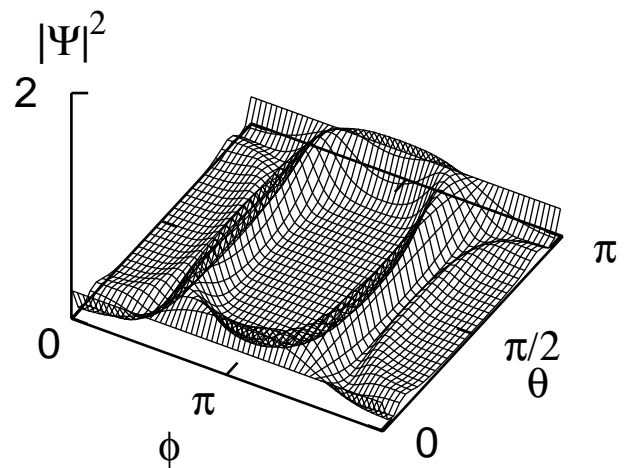
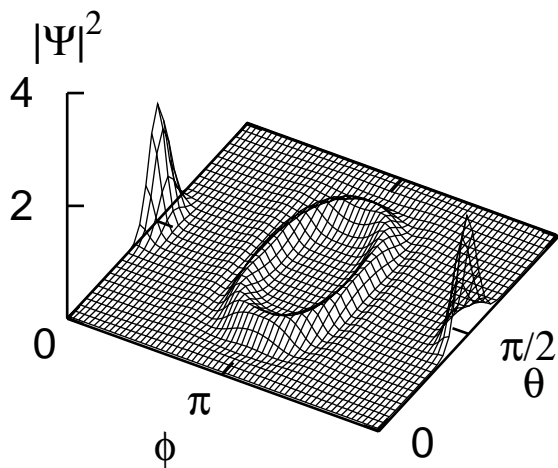
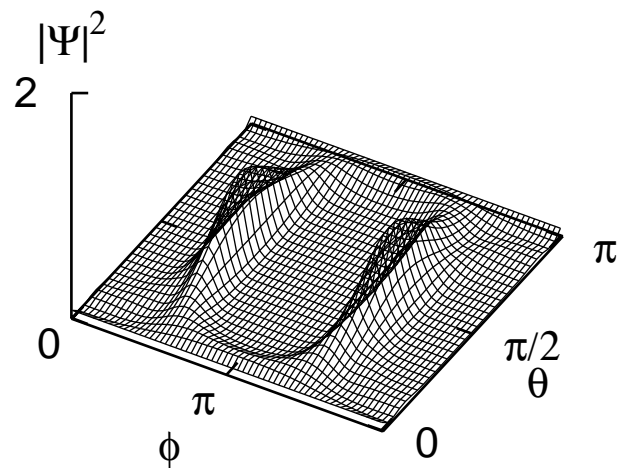
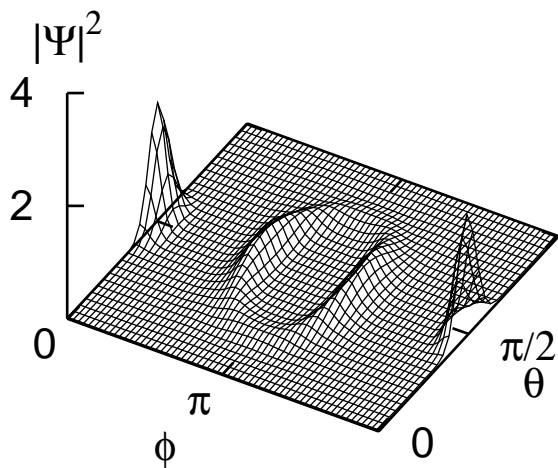
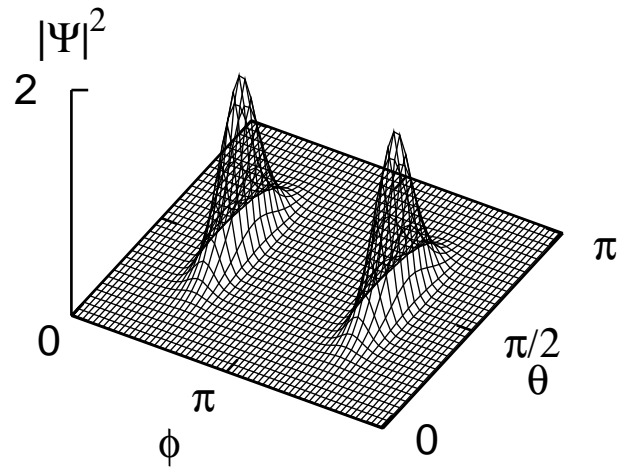
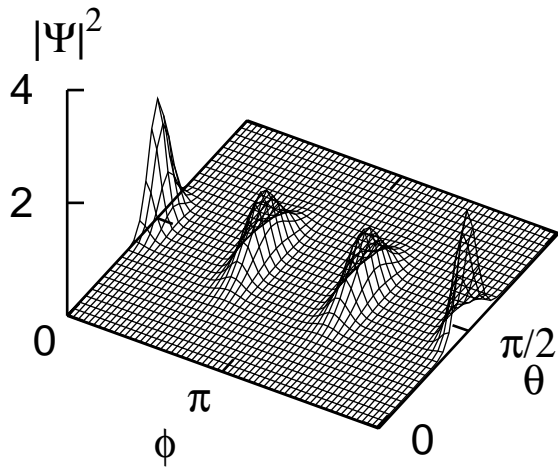
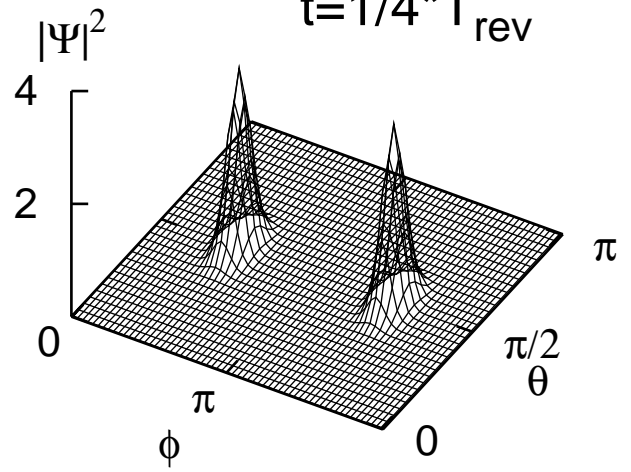
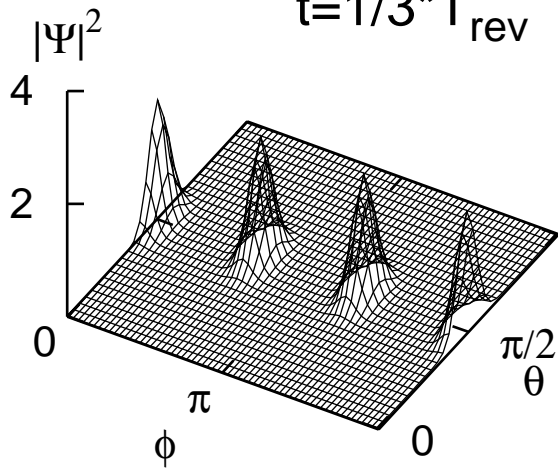
$N^*\eta=20$



N=20

$t=1/3 \cdot T_{\text{rev}}$

$t=1/4 \cdot T_{\text{rev}}$



$N=20 \quad \eta=0.5$

